REVIEW

Check for updates

Comparing total chemical synthesis and total biosynthesis routes to fungal specialized metabolites

Dong-Song Tian, [iD] [a] Xiao Zhang [iD] *[a] and Russell J. Cox [iD] *[b]

Covering the period 1965–2024

Total synthesis has been defined as the art and science of making the molecules of living Nature in the laboratory, and by extension, their analogues. At the extremes, specialised metabolites can be created by total chemical synthesis or by total biosynthesis. In this review we explore the advantages and disadvantages of these two approaches using quantitative methodology that combines measures of molecular complexity, molecular weight and fraction of sp^3 centres for bioactive fungal metabolites. Total biosynthesis usually involves fewer chemical steps and those steps move more directly to the target than comparable total chemical synthesis. However, total biosynthesis currently lacks the flexibility of chemical synthesis and the ability to easily diversify synthetic routes.

1. Introduction

The production and use of specialized metabolites (SM) has long been important to human society and their value in healthcare, agriculture and other fields is undeniable. At the present time there are three main ways by which such compounds may be obtained. First, they are obtained directly from producing organisms; secondly they may be produced by total chemical synthesis;[1] and third, they may be produced by total biosynthesis.[2] Combinations of these strategies may also

[a]*College of Pharmaceutical Sciences, Southwest University, 400715 Chongqing, China. E-mail: zhangxiao023@swu.edu.cn; dstian@swu.edu.cn*

[b]*Institute for Organic Chemistry, Leibniz University of Hannover, Schneiderberg 38, 30167 Hannover, Germany. E-mail: russell.cox@oci.uni-hannover.de*

be effective. For example the production of paclitaxel[3] and artemisinin[4] is achieved by a combination of biosynthesis and chemical synthesis (*i.e.* semi-synthesis).[5]

Each production method comes with its own advantages and disadvantages. For example, production of many SMs by plants allows the methods of horticulture or agriculture to be deployed, for example in the cases of morphine[6] and the cannabinoids.[7] However, harvest of wild organisms may be ecologically damaging, as in the case of the pacific yew that produces paclitaxel in low amounts. In terms of domesticated plant production of SMs, variable weather, and pressures on land and water resources can mean that agricultural production competes with food production. Additionally, many compounds obtained directly from host organisms may have imperfect biological properties and require further chemical modification. In the case of microorganisms, production by fermentation can often be optimal, such as the production of beta-lactams in 100 g L^{-1} titres.[8] However, many organisms produce SMs much less well.

In contrast, total chemical synthesis is highly flexible and almost any desired compound can be produced, especially the structurally modified analogues of SMs and natural metabolites that are toxic to the host organisms. Until now, chemical synthesis as a predominate tactic has contributed tremendously to life-saving medicine discovery as well as fundamental chemical manufacturing. But chemical synthesis routes very often feature prohibitively high step counts, and they are highly carbon intensive, especially for structurally complex SMs with fused polycyclic skeletons and multiple stereocenters. The urgent requirement to significantly curtail carbon emissions

places additional pressures on the use of total chemical synthesis for SM production.[9,10]

Total biosynthesis routes can be inherently energy- and carbon-efficient because biological production normally involves a single process, followed by extraction and purification. Biosynthetic routes can be used for production of SMs where the pathways are well understood and where suitable host organisms are available and easily manipulated, but these features are not always available. Furthermore, routes to known SMs can be inflexible, and it is currently difficult to expand the footprint of biosynthetic pathways to encompass the synthesis of congeners that don't exist in nature.

It would therefore be useful to find a systematic way in which chemical and biological production of SMs could be directly compared. Recent advances in informatic methodology have focussed on determining measures of the complexity of individual molecules. Such measures can include the molecular weight of metabolites (MW), the fraction of sp^3 hybridised carbon atoms (Fsp^3)[11,12] and the so-called complexity index (C_m).[13,14] No single measure is perfect, but the combination of

all three of these measures can be useful for capturing the complexity of individual compounds, or for observing how complexity changes during a synthetic pathway.[15] The rapidity by which complexity is gained stands as a proxy of pathway efficiency: efficient pathways should create complex SMs in as few processes as possible. In particular, 3D plots of complexity values allow visualization and comparison of different synthetic routes in a chemical space in which distances represent chemical changes in complexity, molecular weight and hybridisation. This allows a direct comparison of different biological and chemical synthetic strategies.

Fungi produce a very broad range of complex and bioactive SMs, and there is a very long history of biosynthetic[16] and chemical synthetic[17] investigations of these compounds. Fungi produce all the major classes of SMs including varied fatty acids and polyketides, peptides, terpenes, alkaloids, and compounds of mixed origin such as meroterpenoids.[18] Much is now known of their biosynthesis, and recent rapid developments in molecular and genetic methods in fungi mean that many more biosynthetic routes have been fully determined. Fungal SMs thus present a rich group of compounds where comparisons between total chemical and total biosynthetic[19] methods can be made directly. In this review we attempt to apply these ideas to a variety of total chemical synthesis and total biosynthesis routes to fungal SMs. For simplicity of discussion we select a range of compounds that reflect the different biosynthetic strategies by which fungi assemble SMs.

1.1 Molecular complexity calculations

Descriptors Fsp^3, C_m (mcbit) and MW (Da) can be used to define molecular complexity. In the following sections we calculated and measured these values for the intermediates of both biosynthetic and chemical synthetic pathways. During biosynthesis, CoA thiolesters (and sometimes carrier proteins) are often precursors and intermediates. However, since coenzyme A and carrier proteins are always regenerated and reused in biological systems, we did not include these moieties in molecular

Dong-Song Tian received his Master degree (2017) in medicinal chemistry from Guizhou University and PhD in microbiological chemistry (2021) under the supervision of Prof. Russell J. Cox at Leibniz University Hannover, Germany. After a short period of postdoctoral research (2022) in the Cox group, he moved back to China. Now he is an assistant professor in the College of Pharmaceutical Sciences at Southwest University,

Dong-Song Tian

China, focusing on genome mining and biosynthesis of bioactive fungal secondary metabolites.

Prof. Xiao Zhang received his BA degree (2009) at Lanzhou University, and earned his PhD (2015) in organic chemistry at Nankai University, China. From 2016 to 2020, he worked as a postdoctoral associate in Prof. Renata's Lab at Scripps Florida. In 2021, He joined the faculty at School of Pharmaceutical Science of Southwest University, China. His research interests focus on biocatalysis and che-moenzymatic synthesis of bioac-

Xiao Zhang

tive natural products.

Russell Cox studied fungal metabolites at the University of Durham for his PhD Post-doctoral periods with Professors Vederas in Edmonton, Hopwood in Norwich and Simpson in Bristol were followed by his appointment at the University of Bristol where he became Professor of Organic and Biological Chemistry. He moved to the Leibniz Universität Hannover in 2013. He was an editorial board member of

Russell J. Cox

Natural Product Reports *until 2012 and has been past chair of the Directing Biosynthesis series of conferences. He is currently co-chair of the editorial board of* RSC Advances *and speaker for the DFG Research Unit 5170 CytoLabs.*

complexity calculations. Likewise, in the synthetic routes, we did not include calculations of the complexity changes in reagents and catalysts. So here we use methyl-thiolesters instead of CoA or ACP thiolesters for molecular calculations. However, since protecting groups are essential to most of the chemical routes, we do include these in the calculations. 3D plots parameterized by Fsp^3, C_m and MW were drawn using Matplotlib,[20] a visualization tool based on the python environment. In all cases discussed below the blue colour indicates the biosynthetic route, while orange represents the chemical synthesis.

2. Fatty acid: sporothriolide

Sporothriolide **1** is the major SM produced by the fungi *Hypomontagnella monticulosa*, *H. spongiphila* and *H. submonticulosa*. It possesses a unique alkyl furofurandione architecture and exhibits potent and specific antifungal activity, (*e.g.* 500 ppm protection against *Botrytis cinerea* infection of pepper seedlings),[21] and it has therefore attracted investigations of its biosynthesis and total synthesis.

The genomes of three sporothriolide producers were sequenced and these revealed genes encoding: two fungal fatty acid synthase components (SpofasA & B); an alkyl citrate synthase (SpoE); a methylcitrate dehydratase homolog (SpoL); a decarboxylase (SpoK); a non-heme iron dioxygenase (SpoG); and hydrolases SpoH and SpoJ. The biosynthetic pathway was fully reconstructed in *Aspergillus oryzae* to produce **1** (Scheme 1A).[22] Decanoyl-CoA **2** is synthesised by SpofasA and SpofasB from acetyl- and malonyl-CoA. SpoE (alkyl citrate

synthase) then catalyses condensation with oxaloacetate to form alkyl citrate **3**. Notably two chiral centres are constructed at this stage by the citrate synthase.

However, the precise stereochemical course of SpoE is still elusive, since presumed intermediate **3** was not observed in the WT host or *via* heterologous expression in *A. oryzae*. Dehydration of tertiary alcohol **3** then leads to the formation of alkene **4**. Next, decarboxylation catalysed by SpoK gives the alkyl itaconic acid **5**. Thereafter, alpha-ketoglutarate dependent oxygenase SpoG mediates two rounds of hydroxylation of the saturated alkyl chain to give **7**. The mono- and di-oxygenised itaconic acids are then spontaneously cyclized to lactones **8** and **1**. However, in the presence of lactonases SpoH and SpoJ, conversion of **7** to **1** was observed *in vivo*.

Total synthesis of sporothriolide has been achieved by Kimura and co-workers.[23] The route started from a mixed anhydride of **9** reacting with lithium oxazolidinone salt **18** to give *N*-acyl oxazolidinone **10**. Then Michael addition to nitroalkene **19** gave **11** as a single diastereomer in 73% yield. Subsequent Sharpless asymmetric dihydroxylation of **11** allowed spontaneous lactonization (5-*exo*-trig) and loss of the chiral auxiliary resulting in **12** (75%). The hydroxy group was then protected as a TES ether **13**, prior to ruthenium tetroxide oxidation to carboxylic acid **14**. This was readily converted to bis-lactone **15** after treatment with aqueous hydrochloric acid. Finally, elimination of HNO_2 led to formation of sporothriolide **1** in 71% yield. Summarily, a seven-step enantioselective total synthesis accomplished the construction of sporothriolide **1** in 21% overall yield.

Construction of a 3D plot that represents the pathways in a chemical space shows that they start at similar positions
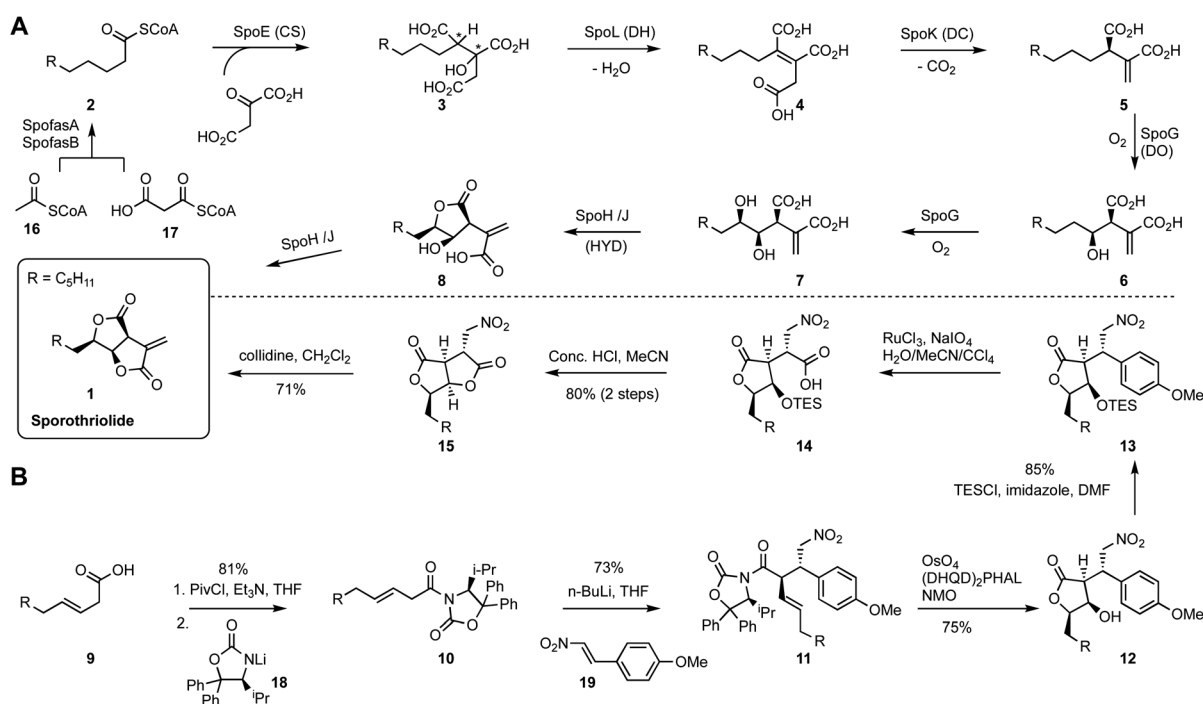
Scheme 1 Sporothriolide 1 syntheses. (A) Biosynthetic pathway; (B) chemical synthesis pathway. FAS: fatty acid synthase, CS: citrate synthase, DH: dehydratase, DC: decarboxylase, DO: dioxygenase, HYD: hydrolase. PivCl: pivaloyl chloride, (DHQD)$_2$2PHAL: hydroquinidine 1,4-phthalazinediyl diether, NMO: 4-methylmorpholine *N*-oxide.

(Fig. 1A). We also calculated the linear distance between each intermediate of the synthesis in the chemical space, in other words, the "chemical distance" of each step using the equation:

$$Distance = \sqrt{(MW_1 - MW_2)^2 + (C_{m1} - C_{m2})^2 + (Fsp_1^3 - Fsp_2^3)^2}$$

Plotting the results *vs.* step number (*e.g.* Fig. 1B) shows that the chemical route usually involves longer steps in the chemical space.
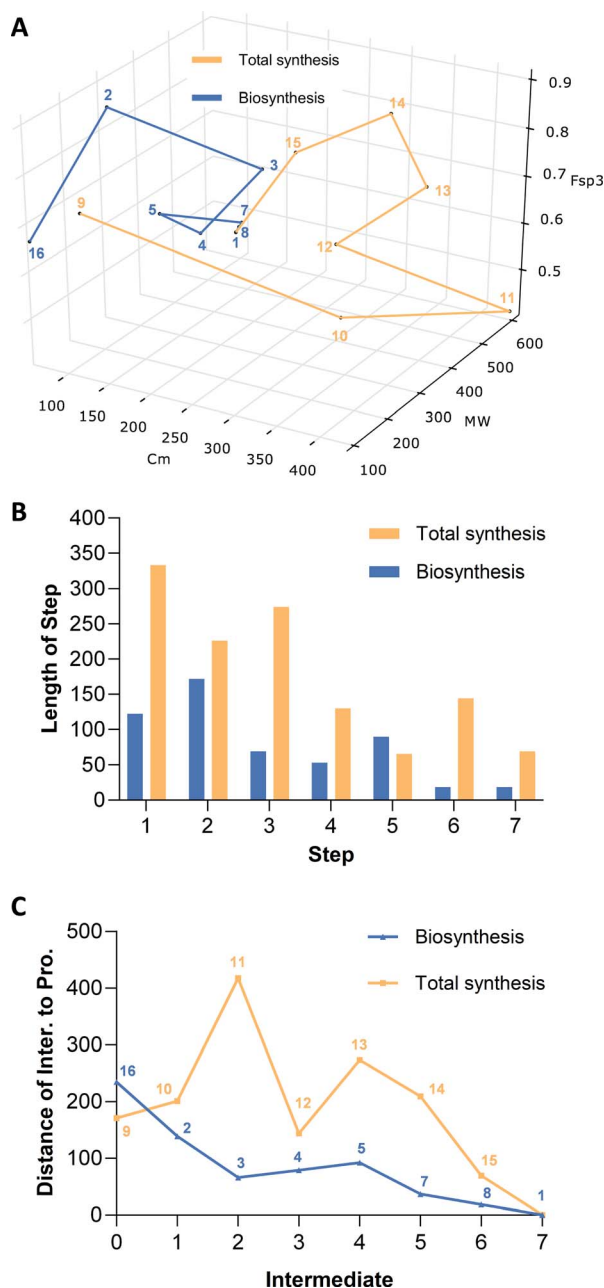

Fig. 1 Chemical space analysis for the production of sporothriolide **1**. (A) The biosynthesis and chemical synthesis of sporothriolide **1** illustrated as a C_m, MW and Fsp^3 parameterized 3D plot; (B) bar chart of distance for each step; (C) line chart of distance of each intermediate to the final product.

Finally, we also measured the distance of each intermediate to the final target and again plotted this *vs.* step (*e.g.* Fig. 1C). In the case of sporothriolide it is clear that while the two pathways to the target both share 7 steps, the chemical synthesis pathway is considerably longer in terms of distance in the complexity space. This is most easily visualised when considering the distance of each intermediate from the target. The biosynthetic pathway reaches the target in steps that usually move each intermediate closer to the target. However, in the synthetic pathway the steps from **10** to **11** and from **12** to **13** both dramatically move the intermediates further away from the target. The step from **10** to **11** involves addition of the *para*-methoxy phenyl unit where all carbons bar one are later removed, while the step from **12** to **13** involves addition of a TES protecting group that is again later removed.

Thus the journey through the 3D chemical complexity space reveals synthetic steps that are atom inefficient because they move the intermediates further away from the target. It is noticeable that the biosynthetic pathway only features two steps where the distance from the target increases: intermediates **3** to **4** to **5**. Once again superfluous atoms are shed during this process, but the intermediates do not move significantly away from the final target.

3. Highly-reduced polyketide: strobilurin A

Strobilurins are antifungal agents isolated from basidiomycetes. The unique β-methoxyacrylate moiety is the toxophore and inspiration for the development of the QoI fungicides widely used in crop protection.[24,25] Syntheses of strobilurins have been achieved by both total chemical synthesis[26,27] as well as by total biosynthesis.[28]

In the biosynthetic pathway (Scheme 2A), benzoyl CoA **21** serves as the precursor to synthesize prestrobilurin **22**. An unusual highly-reducing PKS (StPKS1), with hydrolase domain and unique C-terminal methyltransferase domain, is responsible for the assembly of *EZE* triene **22** using malonyl CoA **17** and *S*-adenosyl methionine (SAM). Then, a flavin-dependent monooxygenase (FMO) Str9 catalyses the oxidative rearrangement of olefin **22** to give aldehyde **24**, presumably *via* intermediate epoxide **23**. Rapid enolization to **25** is followed by two SAM-mediated methylations, firstly by Str2 acting at the carboxyl group, followed by Str3 acting at the enol to obtain strobilurin A **20**.[29]

The chemical synthesis of strobilurin A started from condensation of cinnamaldehyde **27** and benzyloxybutanimine to afford dienal **28** (Scheme 2B). Reduction with NaBH$_4$ in ethanol gave dienol **29**, and subsequent *O*-tosylation and reduction gave **30**. Removal of the benzyl protection then gave **31**. Oxidation with IBX and Pinnick oxidation gave carboxylic acid **33**, which was further methylated to ester **34**. Finally, treatment with base and methyl formate followed by dimethyl sulfate gave strobilurin A **20**.

In comparison the two routes differ significantly in step-count. The biosynthetic route is particularly short, requiring
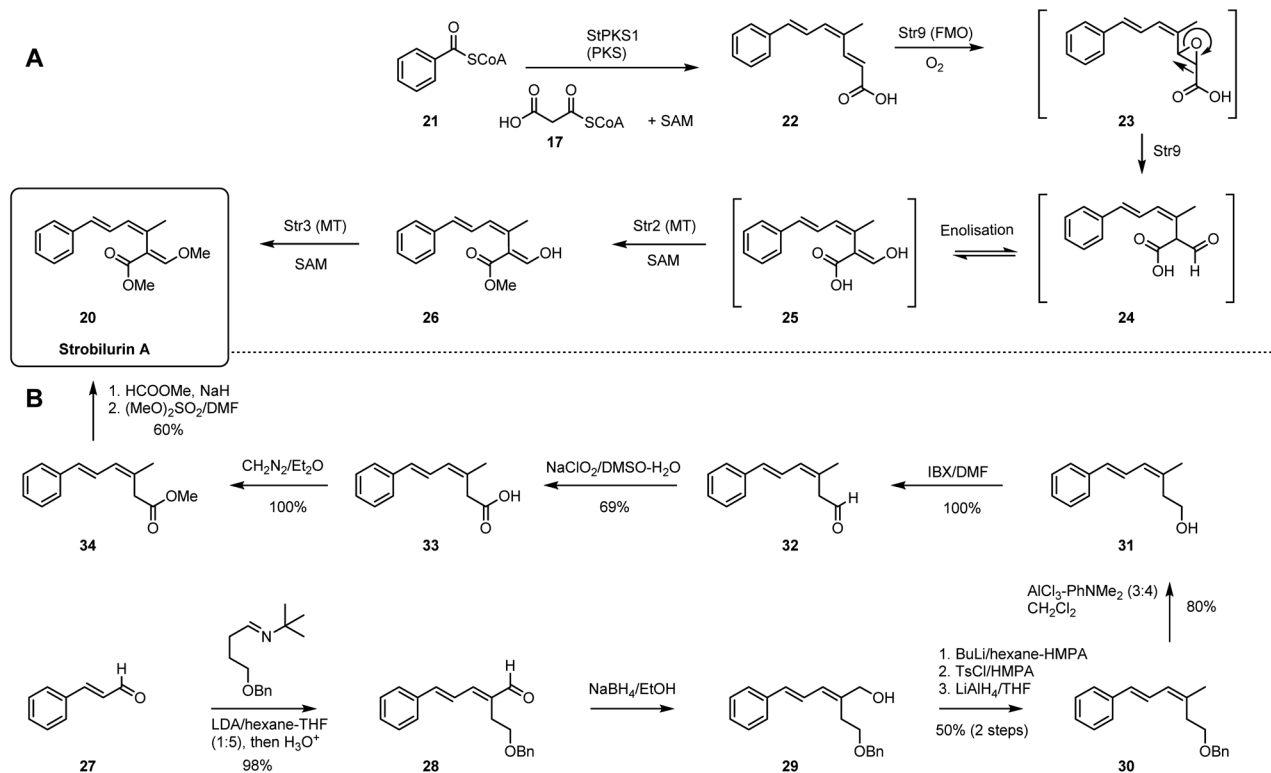
Scheme 2 Strobilurin A **20** syntheses. (A) Biosynthetic process; (B) total chemical synthesis. PKS: polyketide synthase, FMO: flavin–dependent monooxygenase, MT: methyltransferase, SAM: S-adenosyl methionine, LDA: lithium diisopropylamide, IBX: o-iodoxybenzoic acid. TsCl: 4-toluenesulfonyl chloride.
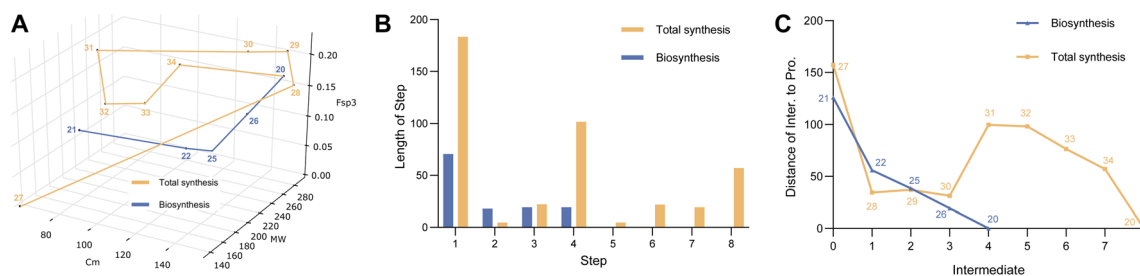

Fig. 2 Chemical space analysis for the production of strobilurin A **20**. (A) The biosynthesis and chemical synthesis of strobilurin A **20** illustrated as a C_m, MW and Fsp^3 parameterized 3D plot; (B) bar chart of distance for each step; (C) line chart of distance of each intermediate to final product.

only a PKS, an oxidative rearrangement and two methylations. In contrast, the chemical synthesis requires eight main steps, although only two of these are carbon–carbon bond-forming steps.

3D Plot of the complexity data shows that the chemical and biological pathways differ significantly. Although the starting points of **21** and **27** are far apart, they are roughly equidistant from the target (Fig. 2C). In the biosynthetic route there are two main processes. First, creation of the polyketide **22** and its oxidative rearrangement move the pathway decisively towards the final C_m value. Then the methylations via **26** increases only the molecular weight and Fsp^3. Each step only moves the route closer to the target (Fig. 2C). In contrast, the total synthesis

route first builds **28** that is close to **20** in all dimensions. But the subsequent seven steps then dramatically move around the complexity space. For example, while intermediate **30** is still close to the final product, step-4 (**30** to **31**) moves C_m by 90 mcbits away from the target and it takes another four steps to recover. This is clearly a feature of the requirement for a protecting group strategy and redox manipulation in the chemical synthesis route.

4. Non-reduced polyketide: citrinin

Citrinin **35** was first discovered in the 1930s and is a widely reported mycotoxin causing food contamination and other

systemic toxic effects.[30] Gene knockout and heterologous expression strategies have fully elucidated the citrinin biosynthetic pathway (Scheme 3A).[31,32] CitS, a non-reducing iterative PKS is responsible for the construction of a trimethylated pentaketide aldehyde **36** from acetyl CoA, malonyl CoA and SAM. Then a non-heme iron oxidase CitB catalyses the oxidation of the methyl of **36** to an alcohol **37**, followed by two sequential oxidations catalysed by oxidoreductases CitC and CitD, to produce aldehyde **38** and carboxylic acid **39**, respectively. The final conversion is performed by CitE, that stereoselectively reduces the 9-ketone and thus facilitates the spontaneous formation of the quinomethide architecture of citrinin **35**.

The chemical synthesis of racemic citrinin was reported by Humpf and co-workers.[33] It commenced with a 2-step preparation of ethyl orsellinate **41** from ethyl acetoacetate **40**. After methylation of the hydroxyl groups to **42**, a *C*-methylation is achieved with methyl iodide under base conditions, to give the ethyl congener **43**. Acetyl chloride was then used to form ketone **44**, and borohydride reduction then allowed spontaneous lactonization to **45**. There then followed a series of reductive steps and deprotections to reach the key intermediate **48**. The stage is now set for the addition of the final two carbons, one by one, to first carboxylate and then formylate the aromatic ring, followed by final oxa-Pictet–Spengler reaction to form citrinin **35**.

Once again, 3D plot of the two pathways reveals interesting differences. The biosynthetic route is short, in terms of step-count with five steps to reach the destination (Fig. 3A). The PKS takes the decisive step in producing **36**, but all steps of the pathway move closer to the target. The chemical synthesis pathway is longer in terms of step count despite the fact that the starting point is close to the biosynthetic starting point. Interestingly the first five synthetic steps to intermediate **45** move the pathway monotonically towards the target. But the next three steps to **46**, **47** and **48** all move the intermediates away from the target in the complexity space. Especially significant is the requirement for a late-stage introduction of two single carbon atoms to **48** that finally brings the synthetic path back on track to the target. It then takes the final two steps of the chemical synthesis to reach the target **35**.

The key differences between the two routes here are that the biosynthetic route installs all the required carbon atoms at the start of the synthesis. This then only leaves redox manipulations and spontaneous cyclisations as requirements to reach the target. In contrast, the synthetic route builds up the carbon-count stepwise. Although additions of carbons in the synthetic route are usually associated with closer approaches to the target, the three reductive steps and the deprotections in the middle of the route required to reach key intermediate **48** contribute to the increased step count overall, while moving the intermediates further away from the target **35**.
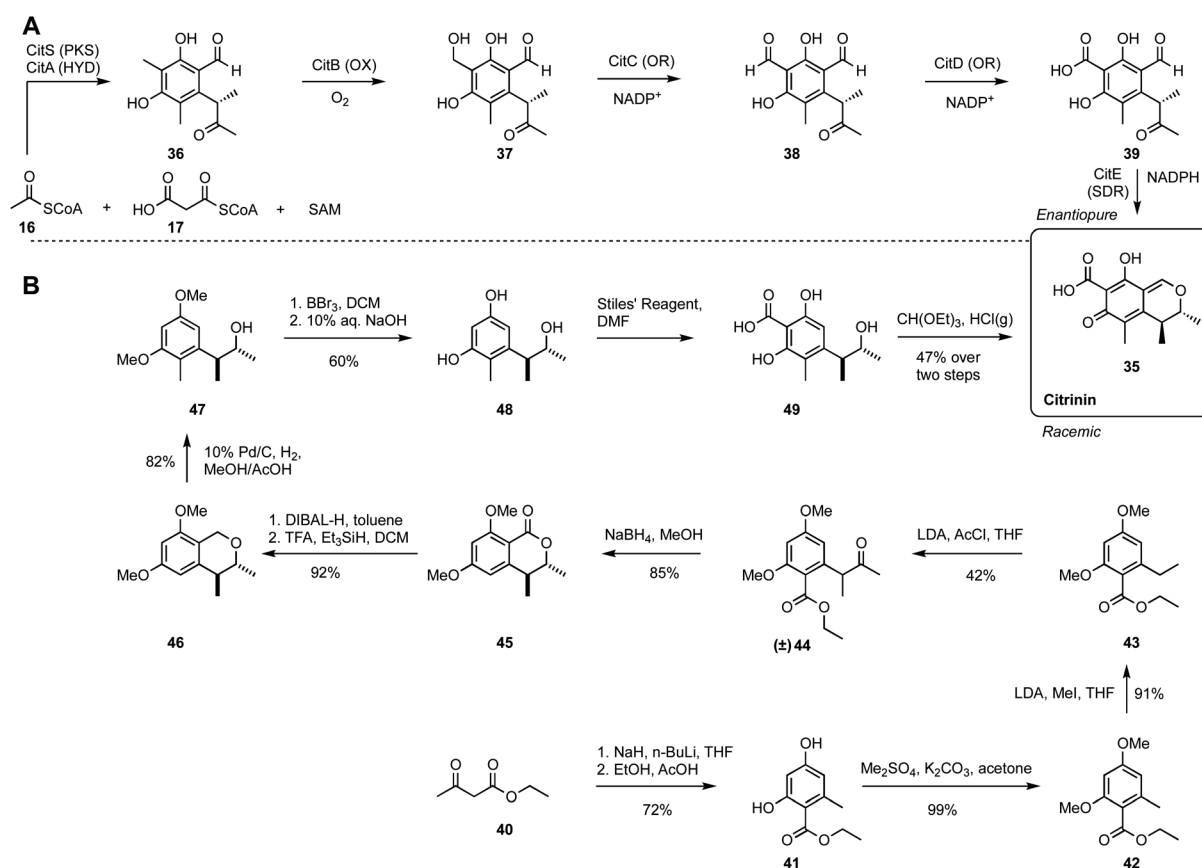
Scheme 3 Citrinin **35** syntheses. (A) Biosynthetic pathway; (B) chemical synthesis pathway. OX: oxygenase/oxidase, OR: oxidoreductase, SDR: short-chain dehydrogenase/reductase. DIBAL-H: diisobutylhydroaluminum, TFA: trifluoroacetic acid.
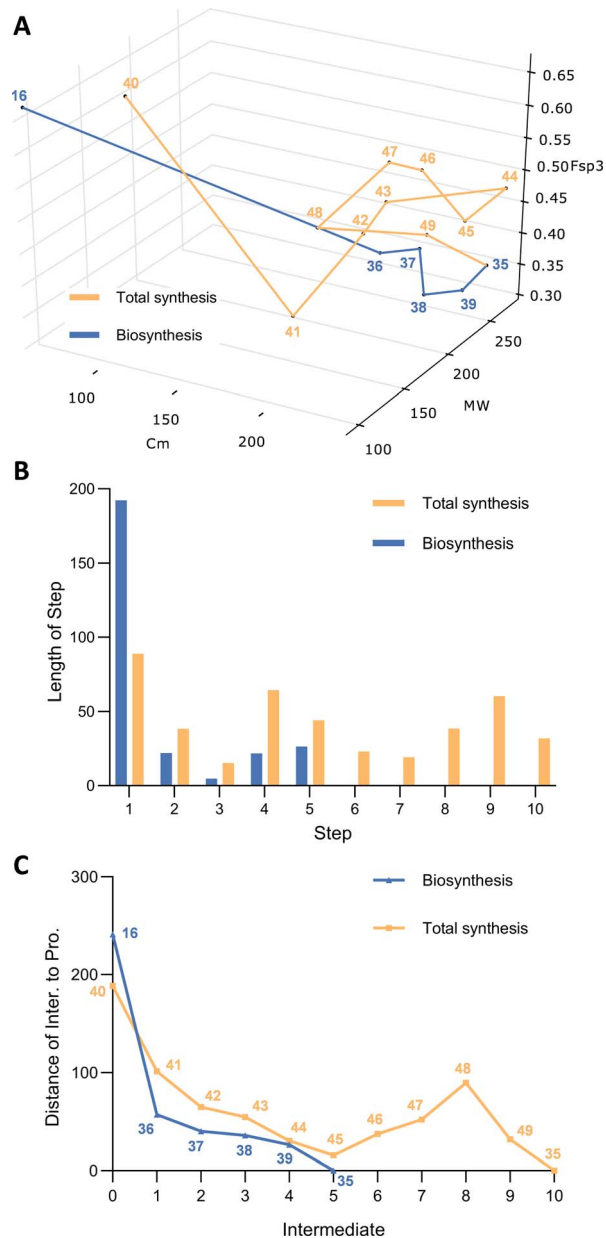
A

B

C

Fig. 3 Chemical space analysis for the production of citrinin **35**. (A) The biosynthesis and chemical synthesis of citrinin **35** illustrated as a C_m, MW and Fsp^3 parameterized 3D plot; (B) bar chart of distance for each step; (C) line chart of distance of each intermediate to final product.

5. Dual PKS system: squalestatin S1

Squalestatins,[34] also known as zaragozic acids,[35] are highly oxidized polyketide derivatives which were discovered as lead compounds for the treatment of hypercholesterolemia in 1990s. Extensive investigations of bioactivities suggested that squalestatins could reduce cholesterol production through the inhibition of squalene synthase. Among them, squalestatin S1 **50**, exhibits nanomolar inhibition of mammalian and fungal squalene synthase, and accordingly displays antifungal properties.[36]

The highly complex caged 4,8-dioxa-bicyclo[3.2.1]octane architecture has attracted constant chemical synthetic investigations.[37,38] Meanwhile, biosynthetic studies have revealed the complete pathway.[39–42] Early isotope labelling experiments revealed the highly reduced polyketide origin of squalestatins, as well as atmosphere and acetate-derived oxygens,[43] while knockout and heterologous expression studies[41,42] revealed the order of the steps and the roles of the biosynthetic enzymes.

Genomic and bioinformatic analysis led to the identification of the squalestatin S1 gene cluster that encodes two highly reducing polyketide synthases (hrPKS) and several oxygenases. Benzoyl CoA **21**, derived by degradation of phenylalanine, is the starter unit for assembly of intermediate **51** by hexaketide synthase SQHKS. Co-expression with a hydrolase (Mfm8) and the citrate synthase (Mfr3) produces the hexaketide citrate **52**. Further introduction of NHI (non-heme iron) oxygenase Mfr1, resulted in the detection of a panel of congeners from LCMS chromatograms, which were consistent with alcohol, ketone, unsaturated ketone and epoxide intermediates on the route to **53**. Since these are derived from the stepwise oxidations of **52** by Mfr1 alone, we refer to the transformations induced by Mfr1 as 'step-2'. Mfr2 then catalyses oxygenations on the oxaloacetate moiety, in which **54** is formed after two rounds of hydroxylation of **53**. A subsequent likely Payne rearrangement to **55**, precedes epoxide opening and cyclisation to yield the key bicyclo unit **56**. We refer to the global conversion from **53** to **56** mediated by Mfr2 as 'step-3'. Next, a copper-dependent oxygenase Mfm1 catalyses allylic alcohol **58** production through rearrangement of **57**, an epoxidized form of **56**. Acetylation of **58** gives **59**. The final step is the O-acylation of **59** to make squalestatin S1 **50**.

Assays conducted in vitro[40] showed that acyl transferase Mfm4 selectively transfers tetraketide CoA thiolester **60** to the 6-hydroxyl of **59**. Mfm4 has a broad substrate scope, catalysing transfer of acyl CoAs from 2 to 10 carbons. Squalestatin tetraketide synthase (SQTKS) is responsible for the construction of the tetraketide moiety in squalestatin S1 biosynthesis based on directed gene knockout and heterologous expression experiments.[39]

The total chemical synthesis of squalestatin S1 **50** has been achieved by Heathcock and co-workers in two overall processes. First, the SM **50** itself was degraded to the relay compound **62** and this was used to develop an 11-step pathway back to **50**.[44] The relay compound **62** was itself synthesised in 25 steps from an advanced precursor **61**,[45] giving a formal total chemical synthesis of 36 steps.

The synthesis of **62** started with 1,6-anhydropyranohexose **61** through a sequence that led to the relay compound **62** that contains the 4,8-dioxabicyclo[3.2.1]octane core (Scheme 4B). Treatment of **62** with pyridinium p-toluenesulfonate afforded cyclic methyl acetal **63** as a mixture of diastereomers. The free hydroxyl of **63** was acylated with α,β-unsaturated acid to yield **64**, while unsaturated acid **73** was supplied from a multiple-step conversion of the starting material tert-butyl acetate. Acetal **64** was hydrolysed to give hydroxy aldehyde **65**, then treated with triethylsilyl chloride to make **66**. Addition of aldehyde **66** with stannane achieved the side chain installation, and the newly formed alcohol **67** was then oxidized by Dess–Martin reagent to
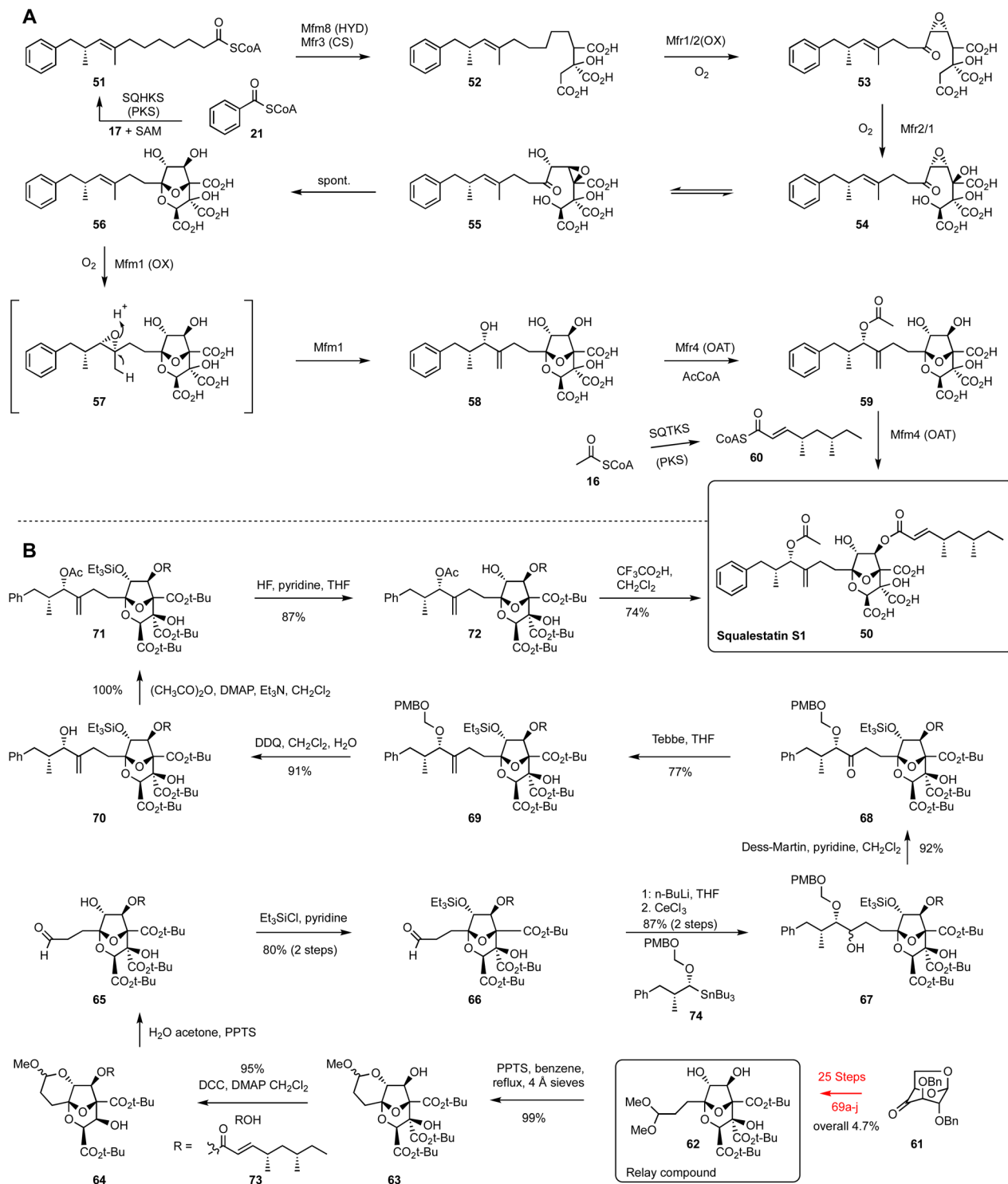
Scheme 4 Squalestatin S1 **50** syntheses. (A) Biosynthetic pathway; (B) chemical synthesis pathway. OAT: O-acyltransferase/acetyltransferase. PPTS: pyridinium tosylate, DCC: dicyclohexylcarbodiimide, DMAP: 4-(dimethylamino)pyridine, DDQ: 2,3-dichloro-5,6-dicyano-1,4-benzoquinone, Tebbe reagent: μ-chloro[di(cyclopenta-2,4-dien-1-yl)]dimethyl(μ-methylene)titaniumaluminum.

yield ketone **68**. The trial in alkene **69** production by employing Wittig reaction resulted in only low yield, however by using Tebbe reaction, a satisfactory synthesis of **69** was achieved. Deprotection and acetylation were conducted smoothly to obtain advanced intermediate **71**. Finally, two-step removal of

the protection groups led to a production of the target squalestatin S1 **50**.

In order to able to sensibly compare the pathways we condensed the synthesis of **62** into a single process. While these steps in combination do move the synthesis closer to the target

in the chemical structure space (Fig. 6A), it should be remembered that the overall yield for this process is a remarkably good 4.7%.

Even starting from the late relay compound **62**, the chemical synthesis of squalestatin S1 **50** requires many more transformations than the biosynthesis (Fig. 4A and B). Once again, the biosynthetic pathway is fairly linear through the chemical space, and each of the seven transformations pushes the intermediates closer to the target. In fact, distance to target decreases almost linearly in the biosynthetic synthesis, whereas

Fig. 4 Chemical space analysis for the production of squalestatin S1 **50**. (A) The biosynthesis and chemical synthesis of squalestatin S1 **50** illustrated as a C_m, MW and Fsp^3 parameterized 3D plot; (B) bar chart of distance for each step; (C) line chart of distance of each intermediate to final product.

the chemical synthesis meanders (Fig. 4C). In particular, chemical steps from **64** to **67** increase mass and complexity through the addition of protecting groups that are later removed in three further steps. These six protection/deprotection steps are required to allow three fairly trivial transformations of the skeleton: oxidation of a secondary alcohol to a ketone and its conversion to the methylene (**67** to **69**); and *O*-acetylation (**70** to **71**) that are the only contributions to the required structure of **50**. The very high efficiency of the biosynthetic pathway is achieved because all of the main skeleton carbons are built-in in the first step, and because of the very high inherent selectivity of the key tailoring functionalisations that include multiple oxygenations, cyclisation and regioselective acylations that do not require any protecting steps.
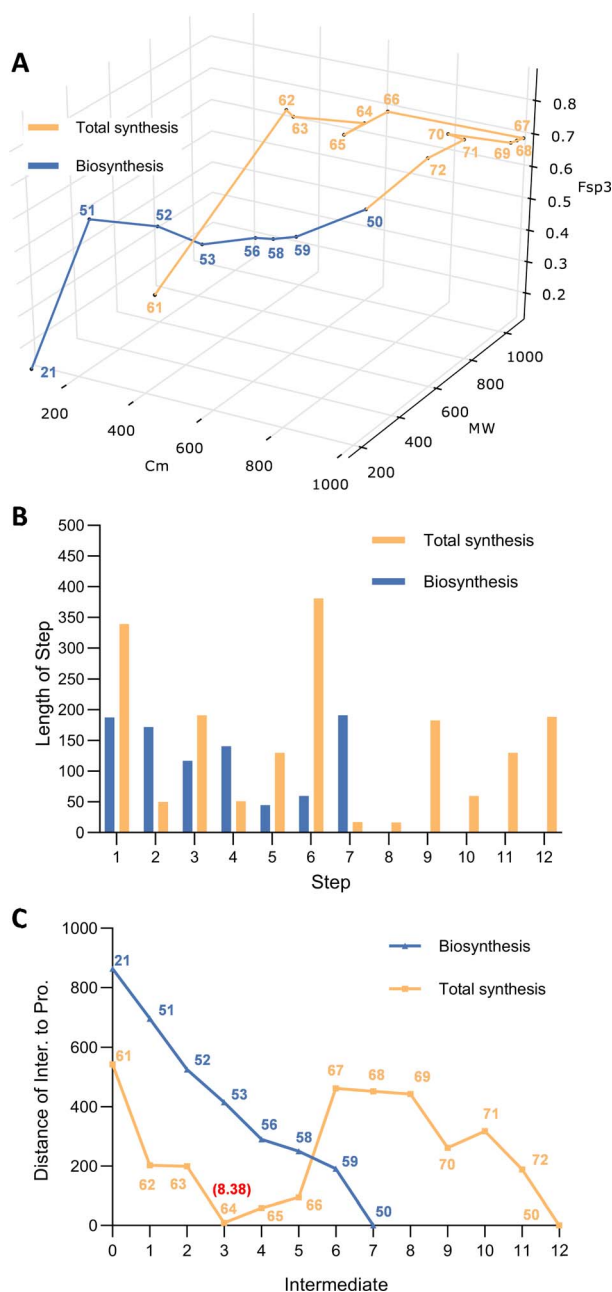
6. Dimeric polyketide: bisorbicillinol

Bisorbicillinoids are biologically active compounds with diverse structures that are isolated from species of *Trichoderma* and other ascomycetes. They possess numerous interesting bioactivities and their fascinatingly complex skeletons have always been attractive synthetic targets. Extensive biosynthetic investigations have completely unveiled the key construction and dimerization process during the biosynthesis of bisorbicillinol **73**.[46–48] The bisorbicillinoid BGC encodes: a highly reducing polyketide synthase SorA; a non-reducing polyketide synthase SorB; two FAD-dependent oxygenases SorC and SorD; as well as transcription factors and transporters. Heterologous expression of functional genes in *Aspergillus oryzae* and bipartite knockout of target genes in *Trichoderma reesei* led to a full understanding of the roles of these enzymes during the biosynthesis.

The first biosynthetic step involves the collaboration of SorA and SorB to assemble the polyketide backbone (Scheme 5). Sorbicillins are often found as mixtures of 2′–3′-saturated and unsaturated forms in the linear side-chains. This is caused by a partially active enoyl reductase (ER) domain of SorA that produces the triketide starter unit **74** for SorB. SorA appears not to be able to fully control the activity of its ER, resulting in mixed products. However, downstream enzymes seem insensitive to this heterogeneity. SorB extends the triketide starter unit **74** three times, methylating the growing chain twice. Finally, reductive release from the PKS gives an aldehyde **75** that undergoes intramolecular Knoevenagel condensation to form the aromatic phenol sorbicillin **76**, that is a critical monomer for the biosynthesis of diverse compounds in this family.

SorC then performs the oxidative dearomatisation of sorbicillin **76** to afford sorbicillinol **77**. The reactive intermediate **77** is both a diene and a dienophile, and it can undergo intermolecular Diels–Alder (DA) cycloaddition to yield the remarkably complex bisorbicillinol **73**. Sorbicillinol **77** is highly reactive, and it can undergo both spontaneous dimerisation (especially during extraction and workup procedures) and enzyme-catalysed Diels–Alder cyclisation, for example by the FAD-dependent SorD. The selectivities of these reactions appears to be affected by solvents in many cases.
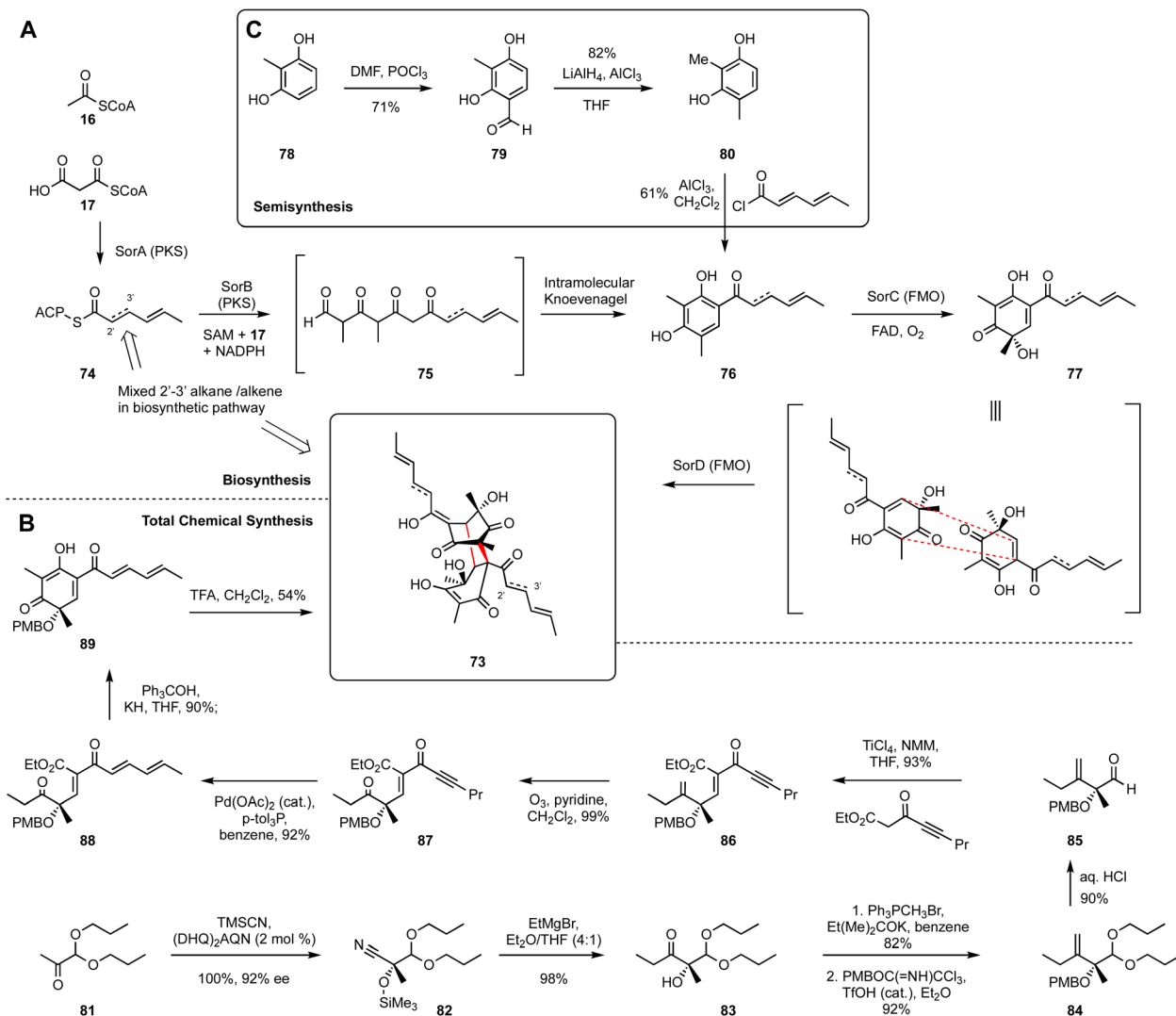
Scheme 5 Bisorbicillinol **73** syntheses. (A) Biosynthetic pathway; (B) chemical synthesis pathway. (DHQ)$_2$AQN: hydroquinine anthraquinone-1,4-diyl diether, TFA: trifluoroacetic acid, NMM: N-methylmorpholine, p-tol$_3$P: tri(o-tolyl)phosphine.

Sorbicillin **76** is formed in essentially a single process from acetyl and malonyl CoA and SAM, and thus the journey through chemical space is roughly linear, with each enzyme-bound intermediates such as **74** already on a direct path to the target. The final dimerization covers more than 50% of the total journey to **73**. Clearly, bisorbicillinol is biosynthesized by nature with extremely high efficiency.

Total chemical synthesis of bisorbicillinol **73** has been achieved by several research groups, for example Nicolaou[49] and Corey *et al.* have reported a 2-step synthesis of the related trichodimerol,[50] but usually as a racemic mixture in low yield. However, Deng *et al.* have reported a highly enantioselective chemical synthesis route to bisorbicillinol **73** using a cyanosilylation as the stereochemistry-defining step, with an overall yield of 12–19%.[51] In this synthesis, acetal ketone **81** was first converted into enantiopure cyanohydrin **82** catalysed by a modified cinchona alkaloid. Next, condensation of nitrile **82** with EtMgBr led to a smooth production of ketone **83**. Then a 1-carbon Wittig

reaction to afford the corresponding methylene, followed by PMB protection of tertiary alcohol using PMBOC(=NH)CCl$_3$ gave PMB-protected ether **84**. The acetal of **84** was hydrolysed under acidic conditions, resulting in aldehyde **85**, which was subjected to Knoevenagel condensation with a readily accessible ynone ester, to yield **86** with high Z selectivity.

Following ozonolysis of the methylene to **87**, the C$_5$ side chain was isomerized to dienone **88**. After numerous trails, Ph$_3$COK was elected as the suitable base for the enolate generation to prompt the intramolecular Claisen–Vorländer cyclisation to PMB-protected sorbicillinol **89**. The final step involves the removal of PMB ether to sorbicillinol **77** with trifluoroacetic acid, and then spontaneous Diels–Alder cycloaddition to the target bisorbicillinol **73** in one pot.

Plotting the biosynthetic and chemical synthetic pathways in 3D gives some insight into the key points of similarity and difference. Once again the biosynthetic pathway reveals its efficiency by its monotonic approach to the target – each

intermediate is closer to the target in the chemical space than the last. The chemical route tends to be more meandering and longer in terms of step count, and in particular intermediates **86–88** do not significantly advance the synthetic pathway, reflecting the requirement to remove a single carbon to reveal a ketone and catalyse an isomerisation. However despite these steps not 'advancing' the synthesis, the overall yield is very high. Thus despite the need for several protective and deprotective steps the overall synthesis is fairly efficient.

Recently, Gulder's group has taken advantages of the highly active enzyme SorC to significantly shorten the chemical synthesis route.[52] SorC offers dual advantages: highly regio-

selective oxidative dearomatisation requires no protecting groups; and very high stereoselectivity means that achiral (and thus easier to make) intermediates are required. Here, simple formylation, LiAlH$_4$ reduction and Friedel–Crafts acylation afford sorbicillin **76** in 3 steps. SorC then catalyses the final oxidation, while spontaneous dimerisation then leads to the target **73**. This route closely follows the biosynthesis and is highly efficient. However, it offers additional advantages because SorC activates various differently-functionalised substrates, in-turn allowing the synthesis of varied analogs of **73** that would be difficult to reach by the biosynthetic route alone. SorC has also been exploited in the synthesis of the non-symmetrical sorbicillactone, again in a remarkably short and efficient process (Fig. 5).[53]
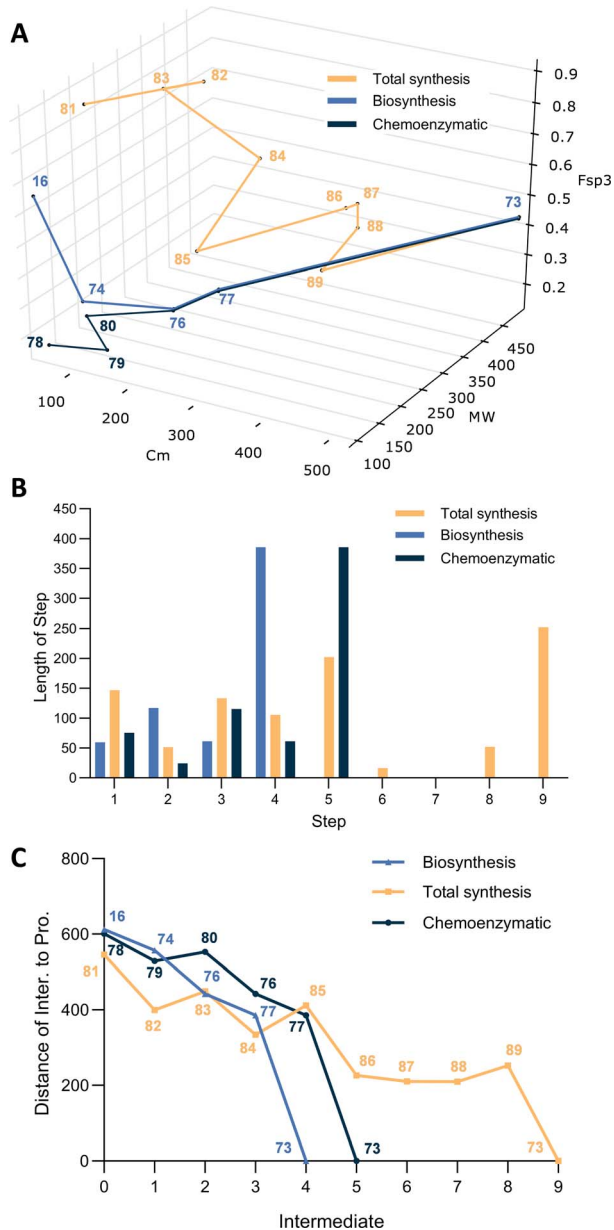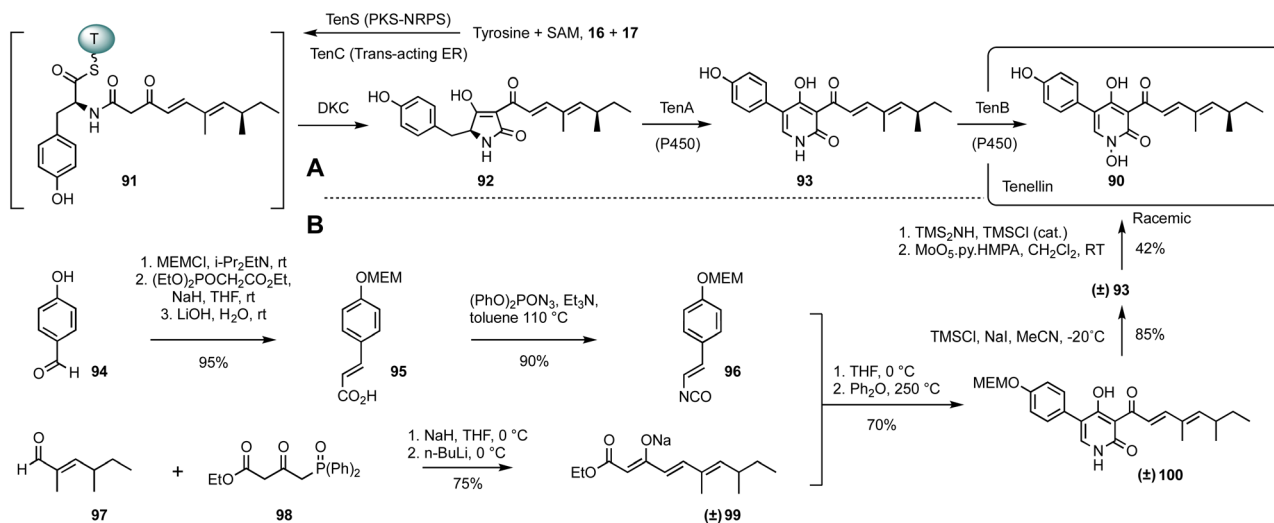
7. PKS-NRPS: tenellin

Tenellin **90** is a 2-pyridone with sub-micromolar cytotoxicity *vs.* human cancer cell lines.[54] It belongs to a large family of fungal SMs that derive from the condensation of an amino acid with a polyketide. Related 2-pyridones such as ilicicolin H possess antifungal activity,[55] and may be responsible for the function of natural biocontrol agents.[56] The 2-pyridones are constructed by oxidative ring-expansion of the corresponding acyl tetramic acids[57] that are also very commonly produced by fungi. This family also includes potent bioactive compounds such as the cytochalasans[58] and mycotoxins such as the fusarins.[59,60] The widespread occurrence, and often potent bioactivity of these compounds has therefore led to numerous total syntheses and detailed investigations of their biosynthesis.

Convergent total synthesis of tenellin was achieved by Rigby and Qabar (Scheme 6).[61] The strategy involves the combination of a vinyl isocyanate **96** with a β-keto ester enolate **99** to yield the tenellin skeleton of pyridone **100**. In order to avoid the side reactions and to increase production yields, removal of MEM protection (2-methoxyethoxymethyl) of **100** to make pretenellin-B **93** was performed first, followed by *N*-hydroxylation to provide the expected racemic tenellin **90**. The requisite vinyl isocyanate **96** was routinely produced from the commercially available 4-hydroxybenzaldehyde **94** in two steps *via* an intermediate carboxylic acid **95**. In parallel, diene keto ester **99** resulted from the Horner–Wittig condensation of hexenal **97** with phosphine oxide **98** in a good yield.

Biosynthesis of tenellin is also a remarkably short process. A hybrid polyketide synthase nonribosomal peptide synthetase (PKS-NRPS), TenS, constructs the tenellin backbone. The PKS is a highly efficient system that builds the required pentaketide from acetate **16**, malonate **17** and SAM using a single iterative module.

Programming of this system has been extensively studied,[62] and effective execution of the programme requires the presence of a *trans*-acting enoyl reductase known as TenC. The completed pentaketide constructed by TenS/TenC is then passed to the NRPS where the condensation (C) domain catalyses the condensation of the ACP tethered pentaketide with thiolation (T) domain bound tyrosine thiolester to afford the ketoacyl amino thiolester **91**. Prior to the condensation process, the

Fig. 5 Chemical space analysis for the production of bisorbicillinol **73**. (A) The biosynthesis and chemical synthesis of bisorbicillinol **73** illustrated as a C_m, MW and Fsp^3 parameterized 3D plot; (B) bar chart of distance for each step; (C) line chart of distances of each intermediate to final product.

Scheme 6 Tenellin **90** syntheses. (A) Biosynthetic pathway; (B) chemical synthesis pathway. DKC: Dieckmann cyclisation domain, PKS–NRPS: polyketide synthase non-ribosomal peptide synthetase, ER: enoyl reductase, P450: cytochrome P450 oxygenase. MEMCl: 2-methoxyethoxymethyl chloride.

tyrosine moiety is initially selected and activated by the adenylation (A) domain, followed by transfer to the T-domain phosphopantetheine arm. A Dieckmann cyclisation is then catalysed by the C-terminal DKC domain to release the enzyme linked **91** from PKS–NRPS system, which generates the first isolatable intermediate pretenellin-A **92** with a typical tetramic acid core. The subsequent oxidative ring expansion from **92** to **93** is carried out by P450 monooxygenase TenA. Finally, a second cytochrome P450 oxygenase, TenB, catalyses the required *N*-hydroxylation to give tenellin **90**.

On the face of it, the two routes to tenellin are rather similar. Both routes approach the target almost monotonically (Fig. 6C) and the chemical synthesis route is only 2 steps longer than the biosynthesis. The chemical synthesis route benefits from the convergent creation of the 2-pyridone, that requires only deprotection and *N*-hydroxylation to reach the target. However, the preceding steps to the pyridone nucleus are rather flattering, appearing to give very quick access to the required precursors. It should be remembered, however, that both **97** and **98** must themselves be made by

multi-step routes, and the overall 5-step sequence is therefore longer in reality.

The biosynthetic route is also extremely efficient. The initial PKS-NRPS TENS/TENC takes advantage of an iterative highly programmed PKS to effectively reach late-stage intermediate **92** in a single step. And, as found in other pathways, the very high selectivity of the late-stage oxidations obviates the need for protecting and redox steps. The TENS/TENC system has also formed the basis for systematic investigations into the programming mechanisms and it has proven possible to control both the chain-length and methylation pattern of the polyketide component.[63–65] Thus, while the biosynthetic pathway already offers very high efficiency, it can also be reengineered to make related compounds such as bassianin.[63]

8. Alkaloid: communesin F

The communesins are a family of indole alkaloids isolated from *Penicillium* species.[66] Structurally, communesins possess seven inter-connected rings, two aminal linkages, and five or six
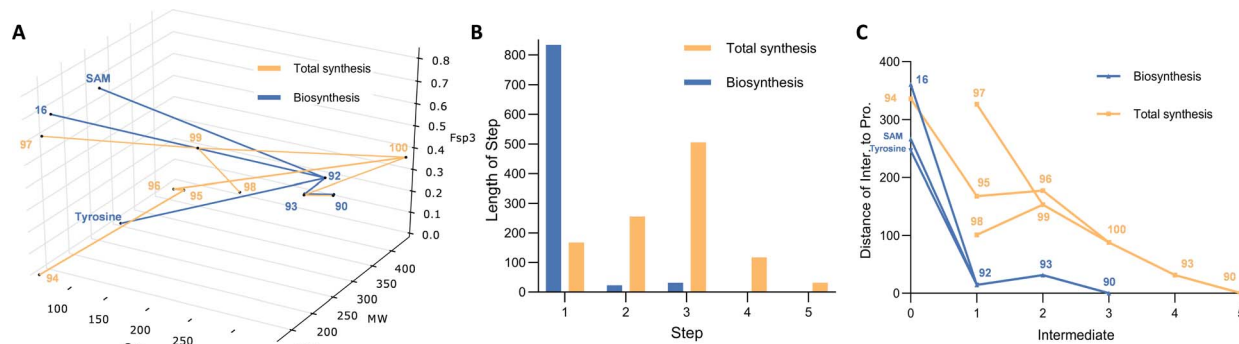

Fig. 6 Chemical space analysis for the production of tenellin **90**. (A) The biosynthesis and chemical synthesis of tenellin **90** illustrated as a C_m, MW and Fsp^3 parameterized 3D plot; (B) bar chart of distance for each step; (C) line chart of distances of each intermediate to final product.

stereocentres. The presence of vicinal quaternary carbon centres makes their chemical synthesis particularly challenging.[67] However, biosynthesis of alkaloids differs from the biosynthesis of polyketides, peptides and terpenes because there is no 'core' synth(et)ase that sets up the skeleton in a single efficient early step. Thus comparison of the biosynthetic and chemical synthetic routes to the same compound is illuminating in a case where nature might be expected to use multiple steps to form the backbone (Scheme 7).

Tryptophan **102** is the precursor for the biosynthetic pathway. Tryptamine **105** is produced by a decarboxylase CnsB. In a parallel pathway, dimethylallylation of tryptophan **102** by the action of 4-dimethylallyl tryptophan synthase (DMATS) CnsF yields **103**, and then oxidative cyclisation gives aurantioclavine **104**. It is known that an FAD-dependent monooxygenase CnsA is responsible for this intramolecular conversion, aided by the catalase CnsD. Biochemical evidence shows that the tryptophan derived units **104** and **105** are then

linked *via* a heterodimeric coupling to afford the heptacyclic scaffold **106** of the communesins.[68] The key catalyst is CnsC, a cytochrome P450 monooxygenase that creates the contiguous quaternary centres.[69] Finally, highly selective *N*-methylation (CnsE) and *N*-acetylation give the target **101**.

Yang and co-workers described the first asymmetric synthesis of communesin F **101**, featuring an iridium catalysed intermolecular cyclization in the first step, such that tetracyclic core **110** was produced in gram scale with excellent stereoselectivity from advanced and protected precursors **108** and **109**.[70]

N-methylation of the indole and removal of TBS protection of **110** afforded **111**, then nitrogen was introduced *via* Mitsunobu displacement of hydroxyl with phthalimide to give protected amine **112**. The olefin originating in **109** then underwent oxidative cleavage, Pinnick oxidation and methylation to yield ester **113**. Standard deprotection of the phthalimide using hydrazine led to a primary amine, then a spontaneous

Scheme 7 Communesin F **101** syntheses. (A) Biosynthetic pathway; (B) chemical synthesis pathway. CSA: camphorsulfonic acid, DIAD: diisopropyl azodicarboxylate, Boc$_2$O: di-*tert*-butyl decarbonate, LiHMDS: lithium bis(trimethylsilyl)amide, MsCl: methanesulfonyl chloride, NMT: *N*-methyltransferase, NAT: *N*-acetyltransferase.

lactamization afforded the pentacyclic scaffold, which was Boc protected to give *N*-Boc lactam **114**. Stereoselective α-allylation and Boc group deprotection afforded alkene **116** which was oxidized to the corresponding aldehyde, then treated with NaBH$_4$ to furnish the primary alcohol **117**. Installation of nitrogen was again performed using phthalimide to make protected amine **118**, followed by a routine deprotection and acylation to **119**.

Next, a Heck reaction installed the butenyl moiety to form an allylic alcohol that was subsequently cyclised into hexacyclic

Fig. 7 Chemical space analysis for the production of communesin F **101**. (A) The biosynthesis and chemical synthesis of communesin F **101** illustrated as a C_m, MW and Fsp^3 parameterized 3D plot; (B) bar chart of distance for each step; (C) line chart of distances of each intermediate to final product.

benzazepine **120** *via* a mesylated intermediate. Under the treatment of LiAlH$_4$, amide **120** was reduced to hemiaminal **121**. Finally, mesylation of **121** to give **122**, which is transformed into a highly reactive iminium intermediate, allowed cyclization to the heptacyclic target **101**.

Evaluation of the molecular complexity during the biosynthetic pathway highlights its remarkable efficiency. In particular the dimerisation of **104** and **105** send the route dramatically towards the target, and only two short steps are required to reach the goal. This is remarkable given that it is achieved by a single catalyst. In comparison the chemical synthesis is both very long (14 steps from fairly advanced precursors) and meandering in the chemical space (Fig. 7A). Ultimately this is the result of having to introduce small groups, or even individual nitrogen atoms, one by one in highly atom inefficient processes. The use of protective groups and frequent requirement for redox manipulations results in a chemical synthesis pathway that does not significantly approach the target over very many steps. Never-the-less the chemical synthesis represents a remarkable triumph of marshalling reactions, atoms, and selectivity towards a highly complex molecular goal.

9. Terpene: pleuromutilin

Pleuromutilin **123** is a tricyclic diterpene that is produced by a narrow family of basidiomycetes in the Clitopilus family.[71] Bioactivity assays revealed the antimicrobial character of pleuromutilin. It inhibits protein synthesis by inhibiting the 50S subunit of the bacterial ribosome.[72] Semi-synthetic derivatives find use as medicines for treatment of infections in poultry, swine and humans. These compounds include lefamulin,[73] tiamulin,[74] valnemulin and retapamulin[75] which possess different 14-*O*-acyl groups compared with pleuromutilin **123**. Activity *vs.* MRSA is particularly important as a response to the rapid growth of drug-resistant infections. Numerous independent chemical syntheses have been reported since Gibbons first 28-step racemic route reported in 1982,[76] including Pronin's 16-step racemic route in 2022.[77] Enantioselective total syntheses have also been reported by the Proctor,[78] Herzon[79] and Reisman groups,[80] and the total biosynthesis has also been reported by Foster and co-workers.[81]

The native host organisms produce **123** on solid substrates in low titres. Foster and co-workers, and the group of Oikawa,[82] both delineated the biosynthetic pathway, and achieved total biosynthesis of pleuromutilin. Genome sequence of *C. passeckerianus* gave rapid access to the seven-gene pleuromutilin BGC and heterologous expression of the component genes in *A. oryzae* achieved the total biosynthesis. The BGC encodes a pathway-specific geranylgeranyl diphosphate synthase (Pl-GGS), a diterpene synthase (Pl-CYC), three P450 monooxygenases (Pl-P450-1, Pl-P450-2, and Pl-P450-3), a short-chain dehydrogenase/reductase (Pl-SDR) as well as an acetyl transferase (Pl-AT).[81] Geranylgeranyl diphosphate **126** is not normally available as an intracellular component, so the pleuromutilin pathway starts with its synthesis from isopentenyl diphosphate **124** (IPP) and farnesyl diphosphate **125**
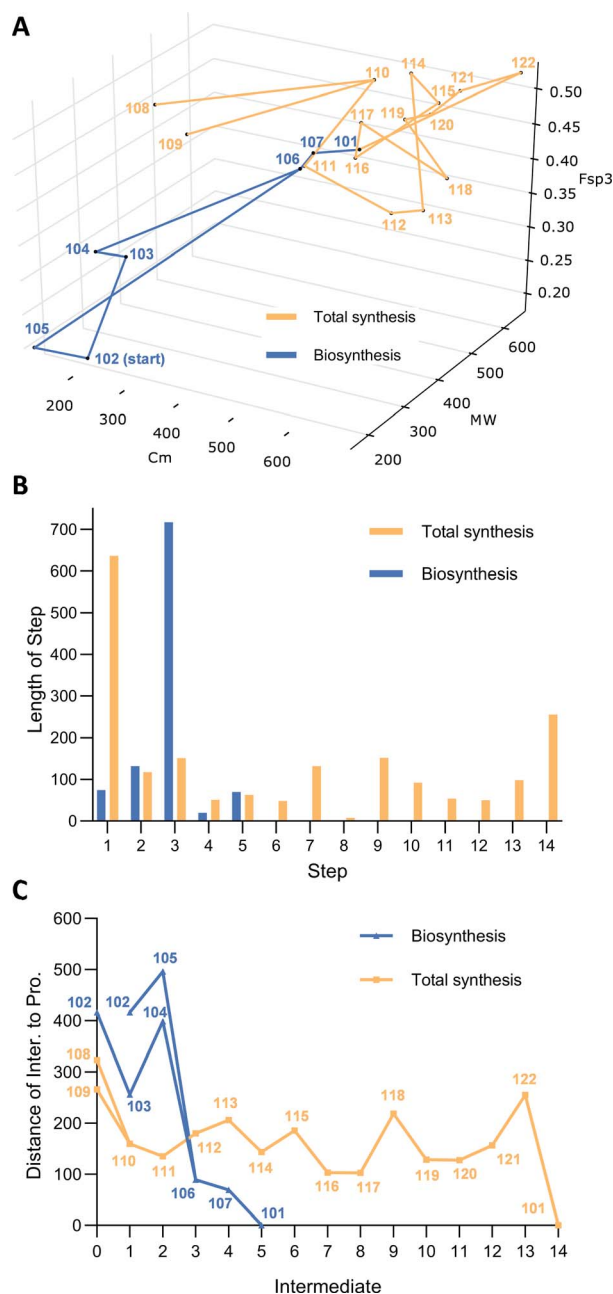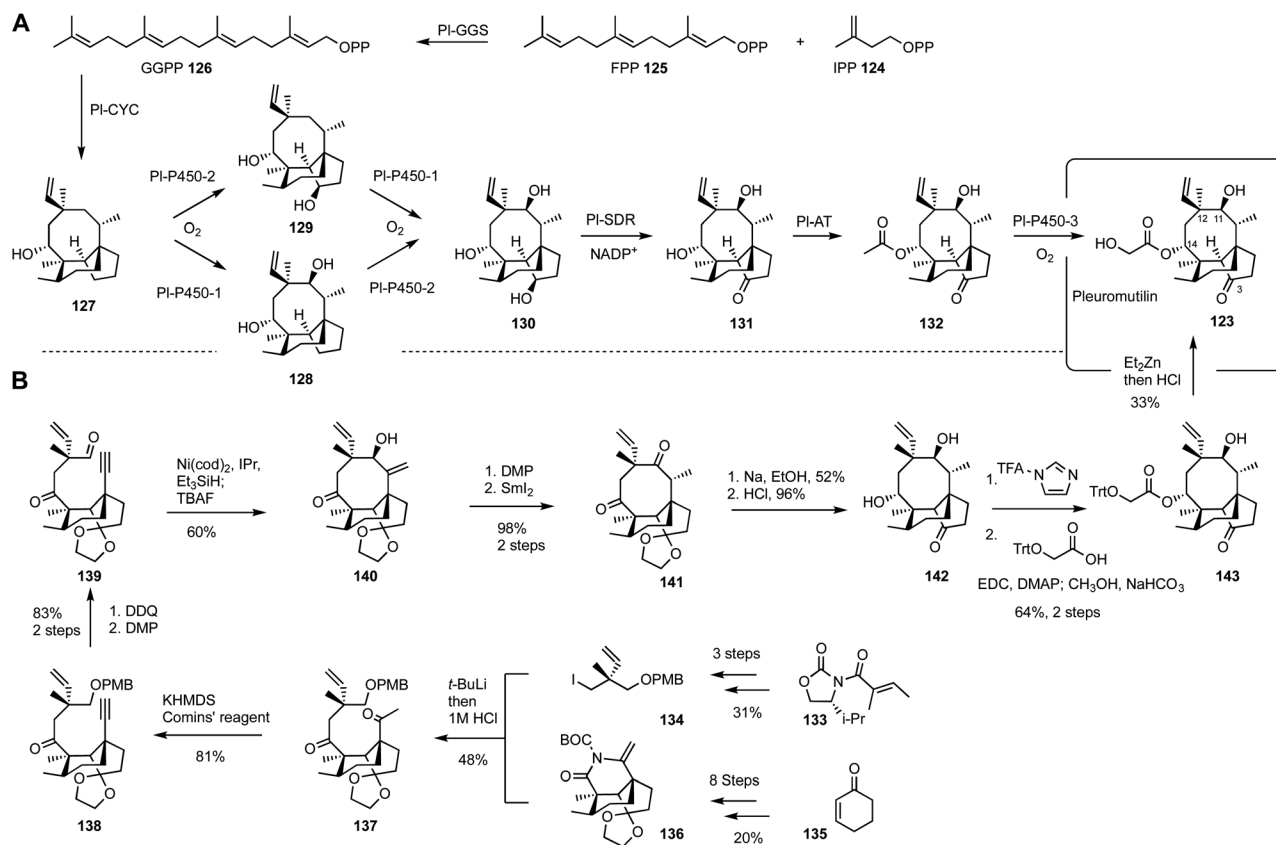
Scheme 8 Routes to pleuromutilin **123**. (A) Biosynthetic pathway; (B) chemical synthesis pathway. Pl-GGS: pleuromutilin geranylgeranyl diphosphate synthase, CYC: diterpene synthase. KHMDS: potassium bis(trimethylsilyl)amide. Ni(cod)₂: bis(1,5-cyclooctadiene)nickel(0), DDQ: 2,3-dichloro-5,6-dicyano-1,4-benzoquinone, IPr: 1,3-bis-(2,6-di-iso-propylphenyl)imidazole-2-ylidene, DMP: Dess–Martin periodinane.

(FPP). A terpene cyclase then creates the tricyclic alcohol **127** in a single step. Two cytochrome P450 monooxygenases can operate in either order, *via* diols **128** and **129** to form triol **130** (Scheme 8).

Oxidation to the ketone **131**, 14-*O*-acetylation and final hydroxylation of the acetyl unit then provides pleuromutilin **123** after an overall 7-step process.[83]

A modular and enantioselective chemical synthesis of pleuromutilins was reported by Herzon and co-workers.[84] The backbone was constructed by coupling of enimide **136** with neopentylic iodether **134**. Compound **136** was achieved in eight steps from commercially available cyclohexanone **135**. In parallel, fragment **134** was prepared *via* asymmetric alkylation of **133** with *p*-methoxybenzyl chloromethyl ether, and subsequent amide reduction as well as iodination.

Comins' reagent was used to convert methyl ketone **137** to acetylene **138**. Deprotection of the PMB (*para*-methoxybenzyl) group followed by oxidation led to the formation of aldehyde **139**. A nickel-based catalyst and triethylsilane was then used for the reductive cyclisation to give the eight-membered cyclic allylic alcohol **140**. Oxidation with Dess–Martin periodinane and samarium diiodide reduction generated α-methyl-ketone **141** with the desired stereochemistry.

Birch reduction of **141** gave the corresponding alcohol, followed by ketal hydrolysis to provide *epi*-mutilin **142**. Stepwise

acylation with trifluoroacetylimidazole and *O*-trityl glycolic acid and routine methanolysis resulted in *O*-trityl-12-*epi*-pleuromutilin **143**. When treated with Et₂Zn, compound **143** was epimerized *via* a retroallylation–allylation process to afford (+)-pleuromutilin **123** in 33% yield, after *in situ* removal of the trityl group. Overall, the route requires 16 steps from cyclohexenone **135**.

Analysis of the two routes in 3D chemical space highlights the similarities of the pathways. Both pathways approach the target monotonically over the first steps, in particular, reaching intermediates **142** and **131** effectively. Although the chemical synthesis appears to do this as effectively as the biosynthesis, this route is already 8-steps into the synthesis from cyclohexenone **135**. As in previous comparisons the biosynthesis also continues to approach its target, the final two steps of acetylation and hydroxylation move the pathway only forwards because of the very high selectivity of the catalysts involved. The final two steps of the chemical synthesis are conceptually similar, involving *O*-acylation with the trityl-protected hydroxyacetate, then deprotection and adventitious 12-epimerization. The large step-lengths for the formation of **143** and **123** in the chemical synthesis reflect the addition and then removal of the large sp³-rich trityl protecting group, illustrating the low atom economy of this process (Fig. 8).
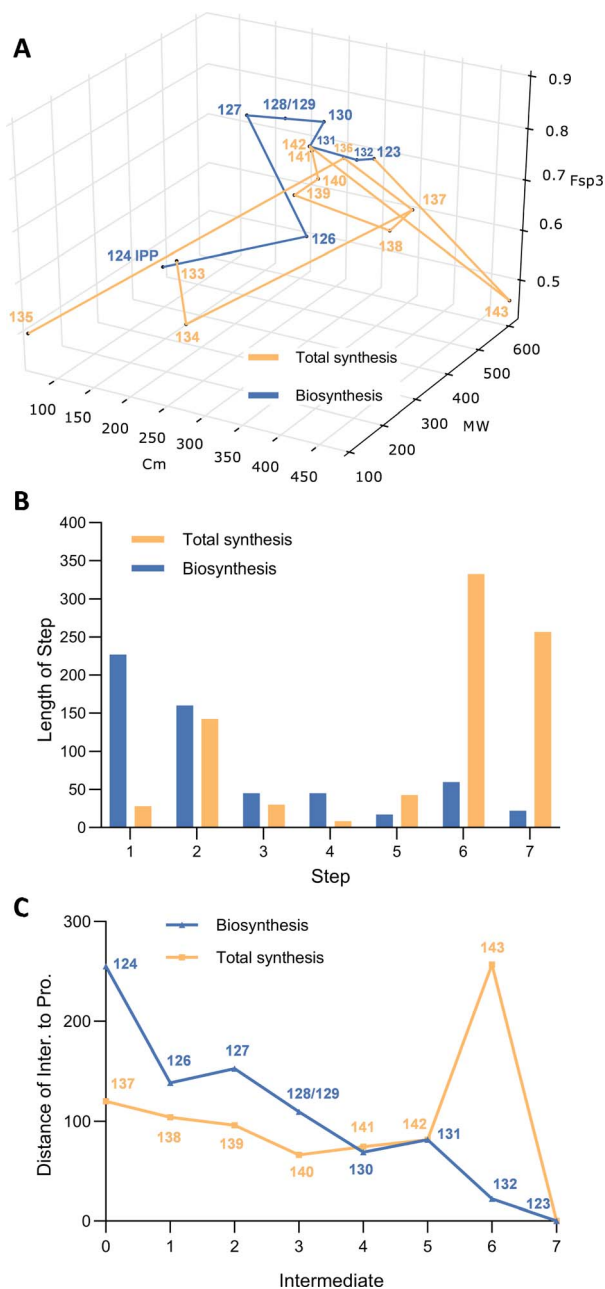
Fig. 8 Chemical space analysis for the production of pleuromutilin **123**. (A) The biosynthesis and chemical synthesis of pleuromutilin **123** illustrated as a C_m, MW and Fsp^3 parameterized 3D plot; (B) bar chart of distance for each step; (C) line chart of distances of each intermediate to final product.

10. Conclusions

Nicolaou and Rigol defined total synthesis as "the art and science of making the molecules of living Nature in the laboratory, and by extension, their analogues".[85] This definition encapsulates both total chemical synthesis, total biosynthesis, and semisynthesis that lies somewhere between. In fact, there is a continuum of methods that nowadays integrate chemical and biological technologies. For example, the deployment of native

Table 1 Productivity of different routes to fungal SMs^a

Compound	Chem. Synth.	Ref.	Biosynth.	Ref.
Sporothriolide	73.5 mg (21%)	23	8 mg L^{-1}	22
Strobilurin A	202 mg (16.2%)	26 and 27	2.6 mg L^{-1}	28
Citrinin	229 mg (4.9%)	33	19.1 mg L^{-1}	31
Squalestatin S1	9.9 mg (1.3%)	44 and 45	Trace	40 and 41
Bisorbicillinol	8.4 mg (27.4%)	51	*	47
Tenellin	* (18.7%)	61	20.4 mg L^{-1}	57
Communesin F	8.6 mg (2.6%)	70	8.3 mg L^{-1}	68 and 69
Pleuromutilin	1.8 mg (0.4%)	84	80 mg L^{-1}	81

^{a} * indicates unmentioned data.

or engineered enzymes from biosynthetic pathways into 'traditional' synthetic routes that often results in significant reduction in step-count of chemical pathways.[86] In this review we have compared the extremes – total chemical synthesis *vs.* total biosynthesis. In each case the outcome is the same – production of SMs (and often their analogs) in the laboratory.

Both total chemical synthesis and total biosynthesis can clearly be used for the production of SMs, but an important question is how much can be made? Direct comparison of absolute yields from synthesis and fermentation processes are not easy to make because they are reported in different units and depend on the scale of production. But reports in the academic literature generally stem from convenient laboratory scale processes (Table 1), yielding amounts between 1 mg and 100s of mg. Normally both processes are relatively easy to scale. For example, a lab-based chemical synthesis of sporothriolide yields more than 70 mg; a 10 L fermentation would also reach similar level. Likewise a 1 L fermentation to produce pleuromutilin would give 80 mg of the desired compound; total chemical synthesis would require a 40× scale-up to reach the same amount. For squalestatin S1, total biosynthesis only yields trace amount, but total chemical synthesis could obtain around 10 mg with an overall yield of 1.3%. In most cases, both sets of processes are within the achievable range.

To compare the routes in more detail we adopted informatic methods pioneered by others[15] that plot synthetic pathways as journeys through 3-dimensional chemical space. The selection of complexity (C_m), Mw (Da) and Fsp^3 is convenient, if arbitrary, and different or better measures may be available. However, these three parameters have the benefit of being easily computed and understood, and their analysis does illuminate aspects of chemical- and bio-synthetic pathways that chemists have 'felt', if not quantified, for many years. Here, we have focussed on examples drawn from fungal SMs, as these compounds are often chemically complex and challenging to construct. However, the analysis could be easily extended to any other class or source of SM.

The analysis shows that in almost all cases the total biosynthetic processes are shorter in terms of step-count, and those steps progress the pathway more quickly towards to target. This is why the integration of enzymes from biosynthetic pathways find favour in chemical synthesis: they usually simultaneously reduce step-count, progress the pathway, and simplify routes. For example, the chemoenzymatic synthesis of

bisorbicillinol **73** allows a dramatic simplification of the early synthetic steps (Scheme 5). In addition, the synthesis is more convergent and does not require protecting groups. In some cases, such as for squalestatin S1 **50**, communesin F **101** and pleuromutilin **123**, the comparison is stark – the biosynthetic processes are dramatically shorter and more effective. In other cases, such as that of sporothriolide **1**, the pathways are more comparable, although the biosynthesis is still shorter and more direct. The analysis in 3D space also allows identification of steps of low atom economy[87] (even in the absence of analysis of the reagents and catalysts themselves). For example, steps from **64** to **67** during the synthesis of squalestatin S1 (already 27 steps 'in' from a complex starter, Scheme 4) involve addition of missing carbons and protecting group manipulations that move the pathway further away from the target. This is avoided in the biosynthetic routes as almost all carbons are present from the start, and protecting groups are not required.

Chemical synthesis is stepwise by its nature and design. It is clear that the step-count can be reduced, often dramatically so, by the introduction of biological catalysts. However, although the total biosynthetic pathways are represented on the page as consecutive synthetic steps, in reality the total biosynthesis is achieved in a single process. This is because all of the enzymes are expressed in a single host organism that produces both the required starting materials, cofactors and enzymes, as well as the mild biological conditions and structures required to support those catalysts: pleuromutilin **123** is produced in *A. oryzae* in a single process that requires a fermentation, an extraction and a purification.[81–83] Such processes are already at the core of modern biotechnology. For example, filamentous fungal hosts produce penicillins at titres of 100 g L^{-1} in well-understood and controlled fermentations.[8] In the case of pleuromutilin **123**, the heterologous production also produces more than 20 times the material produced by the wild-type species because of the way in which the pathway expression is controlled.[81] In the case of communesin F both lab-scale total chemical synthesis and lab scale total biosynthesis yield around 8 mg of the desired compound. However, the biosynthetic process requires a single fermentation, extraction and purification, while the total chemical synthesis requires 14 separate chemical processes. It is thus clear that total biosynthesis dramatically reduces step-counts compared to chemical synthesis, and it is also appropriate for scale-up because the technology for producing SMs by fermentation is already very mature.

Each synthetic step or process requires energy for heating or cooling, but also for the production of solvents, substrates, reagents, ligands and catalysts. Efficiency of synthesis will very likely become of the highest importance in the coming years as the imperative to reduce or remove carbon emissions becomes essential and as fossil-derived carbon becomes rarer and more expensive. Trost argued nearly 30 years ago that atom economy is of key importance,[87] and since then focus on the development of new catalytic methodology has often improved the chemical economy of individual steps, and reduced the number of steps required. For example, Pronin's modern 16-step total chemical synthesis[77] of pleuromutilin **123** is roughly half the length of Gibbons' 1982 route,[76] representing a very significant improvement in efficiency. However, the chemical synthesis route is still 15-steps longer than the total biosynthesis. In a scenario where the requirement to decarbonise is urgent, total biosynthesis becomes a highly attractive way to produce the known SMs while minimising energy consumption and carbon emissions. A further advantage is that once a producing host has been constructed it need not be constructed again: it will continue to produce the desired SM continuously. Total chemical synthesis, on the other hand, has to be repeated to produce more material.

The second element of Nicolaou and Rigol's[85] definition of total synthesis, however, is challenging: "and by extension their analogues" is something that total chemical synthesis can do easily. The measures and analysis of the synthetic pathways used here don't consider the flexibility of pathways. For example, Herzon's pleuromutilin **123** synthesis allows easy diversion to various structural analogs, many of which are biologically active.[84] On the contrary, total biosynthesis produces pleuromutilin itself (and its precursors) very effectively, but while variation of the pathway to produce new derivatives is possible,[88] it remains limited.

This requirement to produce new compounds is clearly a major challenge for the emerging practice of total biosynthesis. Total chemical synthesis can, in principle (and often in practice), produce any given target. It does this at the cost of energy and steps, but it is possible. At present, total biosynthesis is highly effective at making any given SM in a single process if the biosynthetic genes can be found, but making analogues will be the next major step. However, progress is being made in the area of fungal metabolites where the concept of mixing and matching genes from related gene clusters already creates libraries of related compounds,[89,90] and where engineering of the core synth(et)ases to change their programmes is possible.[62]

For example, total biosynthesis has recently been used to produce focussed libraries of tropolone meroterpenoids that are currently difficult to obtain by total chemical synthesis.[89] In the case of the parent compound xenovulene A,[91] no total chemical synthesis has yet been reported, but combination of genes from the xenovulene, eupenifeldin and pycnidione BGCs allows rational total biosynthesis of new metabolites. Likewise, our group,[90] and Oikawa, Minami and Liu and coworkers[92] have recently reported the diversification of aristolochene-derived SMs using total biosynthesis as the key methodology. In these ways total biosynthesis starts to approach the flexibility of total chemical synthesis, while retaining the advantages of being single processes.

In the future, incorporation of engineered enzymes from directed evolution[93] and the construction of entirely fabricated biosynthetic gene clusters should allow the construction of a much wider range of compounds by total biosynthesis. The goal will be for total biosynthesis to match the flexibility of total chemical synthesis while maintaining the advantages of efficiency.

11. Author contributions

The review was conceptualised by RJC and DST. DST made the calculations. DST and XZ prepared the initial draft and diagrams, and all authors contributed to the polishing of the MS.

12. Conflicts of interest

There are no conflicts to declare.

13. Acknowledgements

14. Notes and references

1 N. Fay, C. Kouklovsky and A. de la Torre, *ACS Org. Inorg. Au*, 2023, **3**, 350–363.
2 R. J. Cox, *Nat. Rev. Chem*, 2024, **8**, 61–78.
3 J. N. Denis, A. E. Greene, D. Guenard, F. Gueritte-Voegelein, L. Mangatal and P. Potier, *J. Am. Chem. Soc.*, 1988, **110**, 5917–5919.
4 J. Turconi, F. Griolet, R. Guevel, G. Oddon, R. Villa, A. Geatti, M. Hvala, K. Rossen, R. Göller and A. Burgard, *Org. Process Res. Dev.*, 2014, **18**, 417–422.
5 J. Kennedy, *Nat. Prod. Rep.*, 2007, **25**, 25–34.
6 S. McAlister, Y. Ou, E. Neff, K. Hapgood, D. Story, P. Mealey and F. McGain, *BMJ Open*, 2016, **6**, e013302.
7 V. Butsic, J. K. Carah, M. Baumann, C. Stephens and J. C. Brenner, *Environ. Res. Lett.*, 2018, **13**, 124017.
8 C. Barreiro and C. García-Estrada, *J. Proteomics*, 2019, **198**, 119–131.
9 P. Gabrielli, L. Rosa, M. Gazzani, R. Meys, A. Bardow, M. Mazzotti and G. Sansavini, *One Earth*, 2023, **6**, 682–704.
10 IPCC, *2023: Synthesis Report. Contribution of Working Groups I, II and III to the Sixth Assessment Report of the Intergovernmental Panel on Climate Change*, ed. H. Lee and J. Romero, IPCC, Geneva, Switzerland, pp. , pp. 35–115, DOI: **10.59327/IPCC/AR6-9789291691647**.
11 F. Lovering, J. Bikker and C. Humblet, *J. Med. Chem.*, 2009, **52**, 6752–6756.
12 W. Wei, S. Cherukupalli, L. Jing, X. Liu and P. Zhan, *Drug Discovery Today*, 2020, **25**, 1839–1845.
13 T. Böttcher, *J. Chem. Inf. Model.*, 2016, **56**, 462–470.
14 T. Böttcher, *J. Mol. Evol.*, 2018, **86**, 1–10.
15 E. M. Landwehr, M. A. Baker, T. Oguma, H. E. Burdge, T. Kawajiri and R. A. Shenvi, *Science*, 2022, **375**, 1270–1274.
16 R. Schor and R. Cox, *Nat. Prod. Rep.*, 2018, **35**, 230–256.
17 B. Reck and P. Spiteller, *Synthesis*, 2015, **47**(19), 2885–2911.
18 Y. Matsuda and I. Abe, *Nat. Prod. Rep.*, 2015, **33**, 26–53.
19 R. J. Cox, *Nat. Rev. Chem*, 2024, 1–18.
20 J. D. Hunter, *Comput. Sci. Eng.*, 2007, **9**(3), 90–95.
21 K. Krohn, K. Ludewig, H. J. Aust, S. Draeger and B. Schulz, *J. Antibiot.*, 1994, **47**, 113–118.
22 D.-S. Tian, E. Kuhnert, J. Ouazzani, D. Wibberg, J. Kalinowski and R. J. Cox, *Chem. Sci.*, 2020, **11**, 12477–12484.
23 M. Kimura, T. Mohri, M. Enomoto, Y. Meguro, Y. Ogura and S. Kuwahara, *J. Org. Chem.*, 2021, **86**, 12475–12479.
24 H. Sauter, W. Steglich and T. Anke, *Angew. Chem., Int. Ed.*, 1999, **38**, 1328–1349.
25 J. M. Clough, *Nat. Prod. Rep.*, 1993, **10**, 565–574.
26 Ya. N. Grigorieva, V. Popovsky, A. Stepanov and E. Lubuzh, *Russ. Chem. Bull.*, 2010, **59**, 2086–2093.
27 V. A. Popovsky, A. V. Stepanov and N. Grigorieva, *Mendeleev Commun.*, 2013, **23**, 190–192.
28 R. Nofiani, K. de Mattos-Shipley, K. E. Lebe, L.-C. Han, Z. Iqbal, A. M. Bailey, C. L. Willis, T. J. Simpson and R. J. Cox, *Nat. Commun.*, 2018, **9**, 3940.
29 K. E. Lebe and R. J. Cox, *RSC Adv.*, 2019, **9**, 31527–31531.
30 B. R. Clark, R. J. Capon, E. Lacey, S. Tennant and J. H. Gill, *Org. Biomol. Chem.*, 2006, **4**, 1520–1528.
31 Y. He and R. J. Cox, *Chem. Sci.*, 2015, **7**, 2119–2127.
32 Y. Xue, C. Kong, W. Shen, C. Bai, Y. Ren, X. Zhou, Y. Zhang and M. Cai, *J. Biotechnol.*, 2017, **242**, 64–72.
33 D. Bergmannniliuc, B. Cramer and H.-U. Humpf, *Mycotoxin Res.*, 2018, **34**, 141–150.
34 P. Procopiou, E. Bailey, M. Bamford, A. Craven, B. Dymock, J. Houston, J. Hutson, B. Kirk, A. McCarthy and M. Sareen, *J. Med. Chem.*, 1994, **37**, 3274–3281.
35 J. D. Bergstrom, M. M. Kurtz, D. J. Rew, A. M. Amend, J. D. Karkas, R. G. Bostedor, V. S. Bansal, C. Dufresne, F. L. VanMiddlesworth and O. D. Hensens, *Proc. Natl. Acad. Sci. U.S.A.*, 1993, **90**, 80–84.
36 K. Hasumi, K. Tachikawa, K. Sakai, S. Murakawa, N. Yoshikawa, S. Kumazawa and A. Endo, *J. Antibiot.*, 1993, **46**, 689–691.
37 K. C. Nicolaou, A. Nadin, J. E. Leresche, E. W. Yue and S. L. Greca, *Angew. Chem., Int. Ed.*, 1994, **33**, 2190–2191.
38 K. C. Nicolaou, E. W. Yue, S. la Greca, A. Nadin, Z. Yang, J. E. Leresche, T. Tsuri, Y. Naniwa and F. de Riccardis, *Chem.–Eur. J.*, 1995, **1**, 467–494.
39 R. J. Cox, F. Glod, D. Hurley, C. M. Lazarus, T. P. Nicholson, B. A. Rudd, T. J. Simpson, B. Wilkinson and Y. Zhang, *Chem. Commun.*, 2004, 2260–2261.
40 B. Bonsch, V. Belt, C. Bartel, N. Duensing, M. Koziol, C. Lazarus, A. Bailey, T. Simpson and R. Cox, *Chem. Commun.*, 2016, **52**, 6777–6780.
41 K. E. Lebe and R. J. Cox, *Chem. Sci.*, 2019, **10**, 1227–1231.
42 N. Liu, Y.-S. Hung, S.-S. Gao, L. Hang, Y. Zou, Y.-H. Chooi and Y. Tang, *Org. Lett.*, 2017, **19**, 3560–3563.
43 C. A. Jones, P. J. Sidebottom, R. J. P. Cannell, D. Noble and B. A. M. Rudd, *J. Antibiot.*, 1992, **45**, 1492–1498.
44 D. Stoermer, S. Caron and C. H. Heathcock, *J. Org. Chem.*, 1996, **61**, 9115–9125.
45 S. Caron, D. Stoermer, A. K. Mapp and C. H. Heathcock, *J. Org. Chem.*, 1996, **61**, 9126–9134.
46 A. al Fahad, A. Abood, K. M. Fisch, A. Osipow, J. Davison, M. Avramović, C. P. Butts, J. Piel, T. J. Simpson and R. J. Cox, *Chem. Sci.*, 2013, **5**, 523–527.

47 L. Kahlert, E. F. Bassiony, R. J. Cox and E. J. Skellam, *Angew. Chem., Int. Ed.*, 2020, **59**, 5816–5822.

48 L. Kahlert, R. J. Cox and E. Skellam, *Chem. Commun.*, 2020, **56**, 10934–10937.

49 K. C. Nicolaou, G. Vassilikogiannakis, K. B. Simonsen, P. S. Baran, Y.-L. Zhong, V. P. Vidali, E. N. Pitsinos and E. A. Couladouros, *J. Am. Chem. Soc.*, 2000, **122**, 3071–3079.

50 D. Barnes-Seeman and E. J. Corey, *Org. Lett.*, 1999, **1**, 1503–1504.

51 R. Hong, Y. Chen and L. Deng, *Angew. Chem., Int. Ed.*, 2005, **44**, 3478–3481.

52 A. Sib and T. A. M. Gulder, *Angew. Chem., Int. Ed.*, 2017, **56**, 12888–12891.

53 J. I. Müller and T. A. M. Gulder, *Commun. Chem.*, 2024, **7**, 39.

54 R. Toshe, E. Charria-Girón, A. Khonsanit, J. J. Luangsa-ard, S. J. Khalid, H. Schrey, S. S. Ebada and M. Stadler, *J. Fungi*, 2024, **10**, 69.

55 Z. Zhang, C. S. Jamieson, Y.-L. Zhao, D. Li, M. Ohashi, K. N. Houk and Y. Tang, *J. Am. Chem. Soc.*, 2019, **141**, 5659–5663.

56 M. L. Shenouda, M. Ambilika and R. J. Cox, *J. Fungi*, 2021, **7**, 1034.

57 L. M. Halo, M. N. Heneghan, A. A. Yakasai, Z. Song, K. Williams, A. M. Bailey, R. J. Cox, C. M. Lazarus and T. J. Simpson, *J. Am. Chem. Soc.*, 2008, **130**, 17988–17996.

58 E. Skellam, *Nat. Prod. Rep.*, 2017, **34**, 1252–1263.

59 Z. Song, R. J. Cox, C. M. Lazarus and T. J. Simpson, *ChemBioChem*, 2004, **5**, 1196–1203.

60 K. Kleigrewe, F. Aydin, K. Hogrefe, P. Piecuch, K. Bergander, E.-U. Würthwein and H.-U. Humpf, *J. Agric. Food Chem.*, 2012, **60**, 5497–5505.

61 J. H. Rigby and M. Qabar, *J. Org. Chem.*, 1989, **54**, 5852–5853.

62 R. J. Cox, *Nat. Prod. Rep.*, 2022, **40**, 9–27.

63 K. M. Fisch, W. Bakeer, A. A. Yakasai, Z. Song, J. Pedrick, Z. Wasil, A. M. Bailey, C. M. Lazarus, T. J. Simpson and R. J. Cox, *J. Am. Chem. Soc.*, 2011, **133**, 16635–16641.

64 X.-L. Yang, S. Friedrich, S. Yin, O. Piech, K. Williams, T. J. Simpson and R. J. Cox, *Chem. Sci.*, 2019, **10**, 8478–8489.

65 K. Schmidt and R. J. Cox, *RSC Adv.*, 2024, **14**, 8963–8970.

66 A. Numata, C. Takahashi, Y. Ito, T. Takada, K. Kawai, Y. Usami, E. Matsumura, M. Imachi, T. Ito and T. Hasegawa, *Tetrahedron Lett.*, 1993, **34**, 2355–2358.

67 P. Siengalewicz, T. Gaich and J. Mulzer, *Angew. Chem., Int. Ed.*, 2008, **47**, 8170–8176.

68 H. Lin, G. Chiou, Y. Chooi, T. C. McMahon, W. Xu, N. K. Garg and Y. Tang, *Angew. Chem., Int. Ed.*, 2015, **54**, 3004–3007.

69 H.-C. Lin, T. C. McMahon, A. Patel, M. Corsello, A. Simon, W. Xu, M. Zhao, K. Houk, N. K. Garg and Y. Tang, *J. Am. Chem. Soc.*, 2016, **138**, 4002–4005.

70 X. Liang, T.-Y. Zhang, X.-Y. Zeng, Y. Zheng, K. Wei and Y.-R. Yang, *J. Am. Chem. Soc.*, 2017, **139**, 3364–3367.

71 A. J. Hartley, K. D. Mattos-Shipley, C. M. Collins, S. Kilaru, G. D. Foster and A. M. Bailey, *FEMS Microbiol. Lett.*, 2009, **297**, 24–30.

72 F. Schlünzen, E. Pyetan, P. Fucini, A. Yonath and J. M. Harms, *Mol. Microbiol.*, 2004, **54**, 1287–1294.

73 J. R. Covvey and A. J. Guarascio, *J. Intern. Med.*, 2022, **291**, 51–63.

74 G. Laber and E. Schütze, *Antimicrob. Agents Chemother.*, 1975, **7**, 517–521.

75 B. Boyd and J. Castaner, *Drugs Future*, 2006, **31**(2), 0107.

76 E. G. Gibbons, *J. Am. Chem. Soc.*, 1982, **104**, 1767–1769.

77 N. J. Foy and S. V. Pronin, *J. Am. Chem. Soc.*, 2022, **144**(23), 10174–10179.

78 N. J. Fazakerley, M. D. Helm and D. J. Procter, *Chem.–Eur. J.*, 2013, **19**, 6718–6723.

79 O. Goethe, M. DiBello and S. B. Herzon, *Nat. Chem.*, 2022, **14**, 1270–1277.

80 E. P. Farney, S. S. Feng, F. Schäfers and S. E. Reisman, *J. Am. Chem. Soc.*, 2018, **140**, 1267–1270.

81 A. M. Bailey, F. Alberti, S. Kilaru, C. M. Collins, K. de Mattos-Shipley, A. J. Hartley, P. Hayes, A. Griffin, C. M. Lazarus, R. J. Cox, C. L. Willis, K. O'Dwyer, D. W. Spence and G. D. Foster, *Sci. Rep.*, 2016, **6**, 25202.

82 M. Yamane, A. Minami, C. Liu, T. Ozaki, I. Takeuchi, T. Tsukagoshi, T. Tokiwano, K. Gomi and H. Oikawa, *ChemBioChem*, 2017, **18**, 2317–2322.

83 T. Tsukagoshi, T. Tokiwano and H. Oikawa, *Biosci., Biotechnol., Biochem.*, 2007, **71**, 3116–3121.

84 S. K. Murphy, M. Zeng and S. B. Herzon, *Science*, 2017, **356**, 956–959.

85 K. C. Nicolaou and S. Rigol, *Nat. Prod. Rep.*, 2020, **37**, 1404–1435.

86 J. Li, F. Li, E. King-Smith and H. Renata, *Nat. Chem.*, 2020, **12**, 173–179.

87 B. M. Trost, *Angew Chem. Int. Ed. Engl.*, 1995, **34**, 259–281.

88 F. Alberti, K. Khairudin, J. A. Davies, S. Sangmalee, C. L. Willis, G. D. Foster and A. M. Bailey, *Chem. Sci.*, 2023, **14**, 3826–3833.

89 C. Schotte, L. Li, D. Wibberg, J. Kalinowski and R. J. Cox, *Angew. Chem., Int. Ed.*, 2020, **59**, 23870–23878.

90 Y. Sun, J. Gerke, K. Becker, E. Kuhnert, B. Verwaaijen, D. Wibberg, J. Kalinowski, M. Stadler and R. J. Cox, *Chem. Sci.*, 2023, **14**, 13463–13467.

91 R. Schor, C. Schotte, D. Wibberg, J. Kalinowski and R. J. Cox, *Nat. Commun.*, 2018, **9**, 1963.

92 Y. Sato, X. Shi, Y. Ye, S. Domon, J. Takino, T. Ozaki, C. Liu, H. Oikawa and A. Minami, *ACS Chem. Biol.*, 2024, **19**, 861–865.

93 H. Renata, J. Z. Wang and F. H. Arnold, *Angew. Chem., Int. Ed.*, 2015, **54**, 3351–3367.